Une méthode volume fini implicite en maillages non-structurés pour les équations de Maxwell 3D en domaine temporel

Victorita Dolean, Stephane Lanteri

INSTITUT NATIONAL DE RECHERCHE EN INFORMATIQUE ET EN AUTOMATIQUE

An implicit finite volume time domain method on unstructured meshes for Maxwell equations in three dimensions

Victorita Dolean — Stéphane Lanteri

N° 5767

Novembre 2005

Thème NUM

ISSN 0249-6399 ISRN INRIA/RR--5767--FR+ENG

An implicit finite volume time domain method on unstructured meshes for Maxwell equations in three dimensions

Victorita Dolean * † , Stéphane Lanteri†

Thème NUM — Systèmes numériques
Projets Caiman

Rapport de recherche n° 5767 — Novembre 2005 — 38 pages

Résumé : Les méthodes numériques existantes pour la résolution des équations de Maxwell en domaine temporel reposent souvent sur un schéma d'intégration en temps explicite et sont par conséquent contraintes par une condition de stabilité qui peut être très restrictive en maillages non-structurés, localement raffinés. La présente étude porte sur la formulation et l'analyse d'un schéma d'intégration en temps implicite couplé à une discrétisation spatiale par une méthode volume fini centrée. Un choix naturel pour obtenir une précision d'ordre 2 en temps est le schéma de Crank-Nicolson. Dans la première partie de ce rapport on étudie les propriétés de la méthode volume fini implicite résultante dans le contexte de la résolution numérique des équations de Maxwell 1D avec différents types de conditions aux limites. On montre notamment que la méthode conserve un équivalent discret de l'énergie électromagnétique lorsque les conditions aux limites expriment une réflexion totale (i.e. en présence de parois métalliques). Lorsqu'une des frontières du domaine est sujette à une condition absorbante, on vérifie que cette énergie décroît. On réalise aussi une étude de la dispersion numérique de la méthode et enfin, on prouve que le problème discret est bien posé. Dans la deuxième partie du rapport, on étend les résultats obtenus en 1D au cas des équations de Maxwell 3D. On conclut en présentant quelques résultas préliminaires sur un cas test académique qui permet de valider la métode proposée.

Mots-clés : équations de Maxwell en domain temporel, méthode volume fini centrée, schéma implicite en temps.

* Laboratoire J.A. Dieudonné, Université de Nice/Sophia Antipolis
† INRIA Sophia Antipolis, projet Caiman

Une méthode volume fini implicite en maillages non-structurés pour les équations de Maxwell 3D en domaine temporel

Abstract: Existing numerical methods for the solution of the time domain Maxwell equations often rely on explicit time integration schemes and are therefore constrained by a stability condition that can be very restrictive on highly refined or unstructured meshes. The present study aims at investigating the applicability of an implicit time integration scheme in conjunction with a finite volume approximation method on unstructured meshes. If one wants to achieve at least second-order accuracy in time, then the most natural choice for the implicit time integration of the semi-discrete Maxwell equations is the Crank-Nicolson scheme. In the first part of the paper, we study some of the mathematical properties of the resulting Implicit Finite Volume Time Domain (IFVTD) method in the one dimensional case using different boundary conditions (metallic, periodic and absorbing boundary conditions). We prove that the IFVTD method globally conserves a discrete form of the electromagnetic energy if the initial boundary value problem is based on metallic or periodic boundary conditions. If an absorbing boundary condition is used then we show that the discrete electromagnetic energy is decreasing. In this one dimensional study, we also prove that the matrix operator characterizing the IFVTD method is invertible. In the second part of the paper, we extend the results of the one dimensional analysis to the three dimensional Maxwell equations. We conclude with preliminary numerical results on a simple academic test case in order to validate the proposed method.

Key-words: time domain Maxwell equations, centered finite volume method, implicit time intergration scheme.

Table des matières

1 Introduction

Numerical simulation of electromagnetic wave problems is very challenging from different points of view : one usually deal with 3D problems, involving complex geometries. In addition, the time and space scales can exhibit localized variations due to the heterogeneity of the propagation media. Therefore the discretization of the underlying mathematical model often results in very large algebraic systems of equations. Despite a lot of efforts in the last twenty years, one is still confronted with the need to develop flexible, accurate and efficient numerical methods for solving a wide range of electromagnetic wave problems corresponding to industrial, military and societal applications. Time domain electromagnetic wave problems are modeled by the so-called time domain Maxwell equations that are usually written as a first order hyperbolic system of partial differential equations. For the numerical treatment of these equations, one can consider different classes of numerical methods, such as finite difference methods, finite element or finite volume methods. The first method developed for these equations was a FDTD (Finite Difference Time Domain) method due to Yee[12]. The main features and advantages of this method are its simplicity (an explicit method defined on cartesian grids) and the energy conservation property, an important ingredient in the numerical simulation of unsteady wave propagation problems. Unfortunately, when dealing with complex geometries, the FDTD method is no longer the best choice since local refinments of the grid, albeit possible in the form subgridding techniques, has an adverse effect on accuracy and efficiency. In particular, locally refined grids induce numerical dispersion that must be corrected by local time stepping strategies which is still an open problem in the framework of time domain numerical methods in general and the FDTD method in particular. Moreover, such local refinment also translates in a very restrictive time step in order to preserve the stability of the explicit leap-frog scheme used for time integration if the FDTD method (but this is of course also the case for other explicit time integration schemes and discretization methods as well).

A new class of numerical methods was nedeed, to take into account both the unstructured nature of the mesh and the hyperbolicity of the equations. Thus, inspired by the ideas developed in computational fluid dynamics, various authors have proposed finite volume schemes, combining upwinding and multi-step, explicit, time integration schemes[10]-[2]-[9]. The stability of such a Finite Volume Time Domain (FVTD) method is studied in [5]. Unfortunately, upwinding creates diffusion and accurate solutions cannot be obtained, especially in long-time simulations. Upwind finite volume formulations have also been developed for time harmonic problems[4]-[1] and similar comments are applicable. More recently, the idea of a centered finite volume scheme was successively developed and studied in [8] and [7] and its convergence properties were studied in [3].

The centered FVTD method proposed in [8]-[7] is non-dissipative and very competitive with Yee's schemes in terms of accuracy on regular tetrahedral meshes. However, since it relies on a leap-frog time integration scheme, it is still constrained by a stability condition that can be very restrictive on locally refined grids. Now, the natural question that arises is : are implicit time integration schemes better adapted for the numerical simulation of Maxwell

equations than the explicit ones when dealing with locally refined grids ? From the stability point of view the answer is obvious. Nevertheless, other properties of the resulting Implicit Finite Volume Time Domain (IFVTD) method need to be analyzed, such as numerical dispersion and inversibility of the linear system, in order to make a fair comparison with the explicit FVTD method. In this work, we study the simplest second order scheme, Crank-Nicolson, coupled to the centered finite volume method proposed in [8]-[7].

In section 2, we first formulate the Crank-Nicolson based IFVTD method in the context of the 1D Maxwell equations. Then, we analyze the energy conservation property and prove the inversibility of the implicit matrix. We study the dispersion properties of the IFVTD method and compare them with the explicit scheme. Numerical results for uniform and non-uniform grids conclude this section. In section 3, we formulate the IFVTD method for the solution of the 3D Maxwell equations and then study the same features as in the 1D case that is, the energy conservation property and the inversibility of the implict matrix. The method is validated using a simple model problem in 3D.

2 The 1D case

2.1 Mathematical model

This study is concerned with the numerical solution of the time domain Maxwell's equations in three space dimensions (heterogeneous linear isotropic medium with no source, with space varying electric permittivity and magnetic permeability) using an implicit finite volume method on unstructured tetrahedral meshes. The electric field $\boldsymbol{E} = (E_x, E_y, E_z)^t$ and the magnetic field $\boldsymbol{H} = (H_x, H_y, H_z)^t$ verify :

$$\begin{cases} \varepsilon(x)\dfrac{\boldsymbol{E}}{\partial t} - \nabla \times \boldsymbol{H} = 0 \\ \mu(x)\dfrac{\boldsymbol{H}}{\partial t} + \nabla \times \boldsymbol{E} = 0 \end{cases} \tag{1}$$

In order to derive a 1D version of the Maxwell's equations (1) we consider that the direction of popagation is $\mathbf{k} = (k, 0, 0)^t$ and that the polarization of the electric field vector is such that $\boldsymbol{E} = (0, 0, E_z)^t$. The polarization of the magnetic field vector is deduced from the cross product $\mathbf{k} \times \boldsymbol{E}$ yielding $\boldsymbol{H} = (0, H_y, 0)^t$. Moreover, we assume that E_z and H_y are functions of x and t. For simplicity, we simply note E instead of E_z and H instead of H_y. Then, the 1D Maxwell equations can be written as :

$$\begin{cases} \dfrac{\partial D}{\partial t} - \dfrac{\partial H}{\partial x} = 0 \\ \dfrac{\partial B}{\partial t} - \dfrac{\partial E}{\partial x} = 0 \end{cases} \tag{2}$$

In eq. (2), D is the electric displacement, E is the electric field, B is the magnetic induction and H is the magnetic field. The above quantities are linked by the following constitutive laws :

$$\left\{ \begin{array}{rcl} D(x,t) & = & \varepsilon(x)E(x,t) \\ B(x,t) & = & \mu(x)H(x,t) \end{array} \right. \tag{3}$$

where $\varepsilon(x)$ and $\mu(x)$ respectively denote the dielectric permittivity and magnetic permeability of the medium that can be expressed in terms of their values in the vacuum (ε_v and μ_v) and relative non-dimensional values ($\varepsilon_r(x)$ and $\mu_r(x)$) :

$$\left\{ \begin{array}{rcl} \varepsilon(x) & = & \varepsilon_v \varepsilon_r(x) \\ \mu(x) & = & \mu_v \mu_r(x) \end{array} \right. \tag{4}$$

Besides, the propagation speed is given by :

$$c(x) = \frac{1}{\sqrt{\varepsilon(x)\mu(x)}}$$

Eq. (2) can be written as :

$$\left\{ \begin{array}{l} \varepsilon(x)\dfrac{\partial E}{\partial t} - \dfrac{\partial H}{\partial x} = 0 \\ \\ \mu(x)\dfrac{\partial H}{\partial t} - \dfrac{\partial E}{\partial x} = 0 \end{array} \right. \tag{5}$$

or, in vectorial, quasi-conservative, form as :

$$B\frac{\partial W}{\partial t} + \frac{\partial F(W)}{\partial x} = 0 \quad \text{for} \quad x \in]a,b[\quad \text{and} \quad t > 0 \tag{6}$$

where :

$$W = \left(\begin{array}{c} E \\ H \end{array} \right) \ , \ B \equiv B(x) = \left(\begin{array}{cc} \varepsilon(x) & 0 \\ 0 & \mu(x) \end{array} \right) \text{ and } F(W) = AW \text{ with } A = \left(\begin{array}{cc} 0 & -1 \\ -1 & 0 \end{array} \right)$$

Various boundary conditions can be imposed at the boundaries $x = a$ and $x = b$. In this work we will study the following combinations :

- metallic boundary conditions both at $x = a$ and $x = b$: $E(a) = E(b) = 0$, i.e the 1D version of the condition $\mathbf{n} \times \boldsymbol{E} = 0$ which is used in the 3D case ($\mathbf{n}$ denotes the unitary outwards normal),
- periodic boundary conditions i.e $E(a) = E(b)$ and $H(a) = H(b)$,
- an absorbing boundary condition at $x = a$ and a metallic boundary condition at $x = b$ (i.e $E(b) = 0$). For what concern the absorbing boundary condition, we make use of the conventions adopted previously i.e :

$$\mathbf{k} = \begin{pmatrix} k \\ 0 \\ 0 \end{pmatrix} \quad , \quad \boldsymbol{E} = \begin{pmatrix} 0 \\ 0 \\ E \end{pmatrix} \quad \text{and} \quad \boldsymbol{H} = \begin{pmatrix} 0 \\ H \\ 0 \end{pmatrix}$$

Therefore, if a first-order Silver-Müller type absorbing condition is imposed at the boundary $x = a$:

$$(\mathbf{n} \times \boldsymbol{E} + c\mu \mathbf{n} \times (\mathbf{n} \times \boldsymbol{H}))(a) = 0$$

then, since $\mathbf{n}(a) = (-1, 0, 0)^t$, we obtain :

$$(\mathbf{n} \times \boldsymbol{E} + c\mu \mathbf{n} \times (\mathbf{n} \times \boldsymbol{H}))(a) = \begin{pmatrix} 0 \\ E(a) \\ 0 \end{pmatrix} + c(a)\mu(a) \begin{pmatrix} 0 \\ -H(a) \\ 0 \end{pmatrix}$$

and thus, we must impose $(E - c\mu H)(a) = 0$.

2.2 Finite volume discretization

The domain $]a, b[$ is discretized using N cells C_j such that $C_j =]x_{j-\frac{1}{2}}, x_{j+\frac{1}{2}}[$ with $\Delta x_j = x_{j+\frac{1}{2}} - x_{j-\frac{1}{2}}$ denoting the volume of C_j for $1 \leq j \leq N$. Note that a cell centered finite volume discretization is adopted (see fig. 1). On each cell C_j, we define the mean value of W denoted by W_j with :

$$W_j = \frac{1}{\Delta x_j} \int_{C_j} W(x, t) dx$$

and we denote by $W_{j\pm\frac{1}{2}}(t)$ the approximate value of W at the interfaces between C_j and $C_{j\pm1}$ that is :

$$W_{j\pm\frac{1}{2}}(t) \approx W(x_j \pm \frac{1}{2}, t)$$

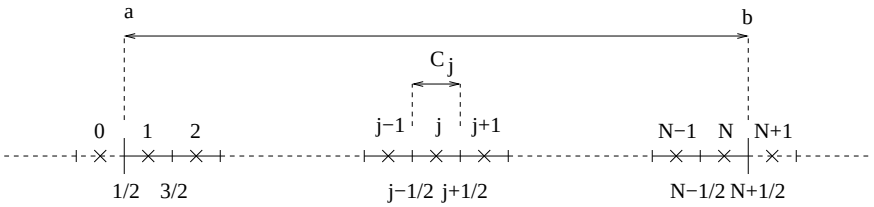

FIG. 1 – Cell centered discretization of the 1D computational domain

Multiplying (6) by a test function $\Psi(x)$ and integrating over $\Omega = [a, b]$ yield :

$$\int_{\Omega} \left(B \frac{\partial W}{\partial t} + \frac{\partial F(W)}{\partial x} \right) \Psi dx = 0 \tag{7}$$

If $\Psi(x)$ is choosen to be the characteristic function associated to the cell C_j (i.e. $\Psi(x) = 1$ if $x \in C_j$ and 0 elsewhere) then (7) becomes :

$$B_j \frac{dW_j}{dt} + \Phi_{j,j-1} + \Phi_{j,j+1} = 0 \tag{8}$$

with :

$$B_j = \begin{pmatrix} \varepsilon_j & 0 \\ 0 & \mu_j \end{pmatrix}$$

where μ_j and ε_j denote values of the coefficients μ and ε that are constant over the cell C_j. In eq. (8), $\Phi_{j,k}$ with $k = \{j-1, j+1\}$ denotes an approximation of the flux between the cells C_j and C_k in the direction of the normal oriented from C_j to C_k. In this study, we adopt a centered approximation for these fluxes following the scheme proposed by Piperno *et al.*[7] :

$$\Phi_{j,j\pm1} = \frac{1}{2}\left(F_j + F_{j\pm1}\right) = \frac{1}{2}\left(AW_j + AW_{j\pm1}\right) = \mp\frac{1}{2}\begin{pmatrix} H_j + H_{j\pm1} \\ E_j + E_{j\pm1} \end{pmatrix} \tag{9}$$

and we thus obtain the following semi-discretization in space :

$$\begin{cases} \varepsilon_j \dfrac{\partial E_j}{\partial t} - \dfrac{H_{j+1} - H_{j-1}}{2\Delta x_j} = 0, \\ \mu_j \dfrac{\partial H_j}{\partial t} - \dfrac{E_{j+1} - E_{j-1}}{2\Delta x_j} = 0. \end{cases} \tag{10}$$

In order to discretize in time the system, we have at our disposal an explicit Leap-Frog scheme which has already been analyzed in [7] :

$$\begin{cases} \varepsilon_j \dfrac{E_j^{n+\frac{1}{2}} - E_j^{n-\frac{1}{2}}}{\Delta t} = \dfrac{H_{j+1}^n - H_{j-1}^n}{2\Delta x_j} \\ \mu_j \dfrac{H_j^{n+1} - H_j^n}{\Delta t} = \dfrac{E_{j+1}^{n+\frac{1}{2}} - E_{j-1}^{n+\frac{1}{2}}}{2\Delta x_j} \end{cases} \tag{11}$$

In the next section we will develop and study an implicit time integration scheme as it is well known that such schemes posesse better stability properties.

2.3 Implicit time integration

The implicit time integration of eq. (8) relies on a Crank-Nicolson scheme :

$$\left\{\begin{array}{rcl} \varepsilon_j \dfrac{E_j^{n+1}-E_j^n}{\Delta t} & = & \dfrac{1}{2\Delta x_j}\left[\left(\dfrac{H_{j+1}^n+H_{j+1}^{n+1}}{2}\right)-\left(\dfrac{H_{j-1}^n+H_{j-1}^{n+1}}{2}\right)\right] \\ \mu_j \dfrac{H_j^{n+1}-H_j^n}{\Delta t} & = & \dfrac{1}{2\Delta x_j}\left[\left(\dfrac{E_{j+1}^n+E_{j+1}^{n+1}}{2}\right)-\left(\dfrac{E_{j-1}^n+E_{j-1}^{n+1}}{2}\right)\right] \end{array}\right. \tag{12}$$

If we denote by $\sigma_j = \dfrac{4\Delta x_j}{\Delta t}$ then (12) can be written as :

$$\left\{\begin{array}{rcl} \sigma_j\varepsilon_j E_j^{n+1} - H_{j+1}^{n+1} + H_{j-1}^{n+1} & = & \sigma_j\varepsilon_j E_j^n + H_{j+1}^n - H_{j-1}^n \\ \sigma_j\mu_j H_j^{n+1} - E_{j+1}^{n+1} + E_{j-1}^{n+1} & = & \sigma_j\mu_j H_j^n + E_{j+1}^n - E_{j-1}^n \end{array}\right. \tag{13}$$

A matrix form of (13) is given by :

$$-AW_{j-1}^{n+1} + \sigma_j B_j W_j^{n+1} + AW_{j+1}^{n+1} = AW_{j-1}^n + \sigma_j B_j W_j^n - AW_{j+1}^n \quad \text{for} \quad j = 1, \cdots, N \tag{14}$$

If $\mathbf{W}^n = (W_1^n \cdots W_j^n \cdots W_N^n)^t$ then a global representation of equations (14) is written as :

$$M\mathbf{W}^{n+1} = P\mathbf{W}^n \tag{15}$$

where M and P are block-tridiagonal matrices defined by :

$$\left\{\begin{array}{l} M_{i,i} = P_{ii} = \sigma_i B_i,\ i = 1..N, \\ M_{i,i+1} = -P_{i,i+1} = A,\ i = 1..N-1, \\ M_{i,i-1} = -P_{i,i-1} = -A,\ i = 2..N. \end{array}\right. \tag{16}$$

2.3.1 Metallic boundaries

Here, we assume that the boundaries $x = a$ and $x = b$ are both considered as metallic and thus, a reflecting condition is imposed to the electric field ($\mathbf{n} \times E = 0$ in the 3D case where $\mathbf{n}$ denotes the unitary outwards normal vector) while no condition is imposed on the magnetic field. For the numerical treatment of these conditions, we make use of ghost cells C_0 and C_{N+1}. Then, in terms of E and H in (2), these conditions translates into :

- $E_0 = -E_1$ and $E_{N+1} = -E_N$ meaning that the flux of E at the boundaries $x = a$ and $x = b$ is set to 0.
- $H_0 = H_1$ and $H_{N+1} = H_N$ meaning H_0 and H_{N+1} are mirror values of H_1 and H_N respectively.

Note that due to the definition of a control volume C_j, it is not necessary to impose a condition on the fluxes $F_{\frac{1}{2}}$ and $F_{N+\frac{1}{2}}$. Then, these conditions must be injected in the expression (13).

– Case $j = 1$

$$\left\{ \begin{array}{lcl} \sigma_1\varepsilon_1 E_1^{n+1} - H_2^{n+1} + H_1^{n+1} & = & \sigma_1\varepsilon_1 E_1^n + H_2^n - H_1^n \\ \sigma_1\mu_1 H_1^{n+1} - E_2^{n+1} - E_1^{n+1} & = & \sigma_1\mu_1 H_1^n + E_2^n + E_1^n \end{array} \right.$$

– Case $j = N$

$$\left\{ \begin{array}{lcl} \sigma_N\varepsilon_N E_N^{n+1} - H_N^{n+1} + H_{N-1}^{n+1} & = & \sigma_N\varepsilon_N E_N^n + H_N^n - H_{N-1}^n \\ \sigma_N\mu_N H_N^{n+1} + E_N^{n+1} + E_{N-1}^{n+1} & = & \sigma_N\mu_N H_N^n - E_N^n - E_{N-1}^n \end{array} \right.$$

Thus, the first and last diagonal 2×2 blocks of M and P must be modified as :

$$\left\{ \begin{array}{lcccl} M_{11} & = & \sigma_1 B_1 & + & C_1 \\ M_{NN} & = & \sigma_N B_N & - & C_N \end{array} \right. \quad \left\{ \begin{array}{lcccl} P_{11} & = & \sigma_1 B_1 & - & C_1 \\ P_{NN} & = & \sigma_N B_N & + & C_N \end{array} \right. \tag{17}$$

where :

$$C_1 = \begin{pmatrix} 0 & 1 \\ -1 & 0 \end{pmatrix} \quad \text{and} \quad C_N = \begin{pmatrix} 0 & 1 \\ -1 & 0 \end{pmatrix}$$

2.3.2 Periodic boundaries

Here, we consider that periodic boundary conditions are applied at the boundaries $x = a$ and $x = b$. This translates into :

$$\begin{array}{l} E_0 = E_N \ \text{ and } \ E_{N+1} = E_1 \\ H_0 = H_N \ \text{ and } \ H_{N+1} = H_1 \end{array} \tag{18}$$

Then, the expressions (13) are modified as follows.

– Case $j = 1$

$$\left\{ \begin{array}{lcl} \sigma_1\varepsilon_1 E_1^{n+1} - H_2^{n+1} + H_N^{n+1} & = & \sigma_1\varepsilon_1 E_1^n + H_2^n - H_N^n \\ \sigma_1\mu_1 H_1^{n+1} - E_2^{n+1} + E_N^{n+1} & = & \sigma_1\mu_1 H_1^n + E_2^n - E_N^n \end{array} \right.$$

– Case $j = N$

$$\left\{ \begin{array}{lcl} \sigma_N\varepsilon_N E_N^{n+1} - H_1^{n+1} + H_{N-1}^{n+1} & = & \sigma_N\varepsilon_N E_N^n + H_1^n - H_{N-1}^n \\ \sigma_N\mu_N H_N^{n+1} - E_1^{n+1} + E_{N-1}^{n+1} & = & \sigma_N\mu_N H_N^n + E_1^n - E_{N-1}^n \end{array} \right.$$

Thus, the following 2×2 blocks must be introduced in the expressions of the matrices M and P :

$$\left\{ \begin{array}{l} M_{1N} = -A \\ M_{N1} = A \end{array} \right. \quad \left\{ \begin{array}{l} P_{1N} = A \\ P_{N1} = -A \end{array} \right. \tag{19}$$

2.3.3 Metallic and absorbing boundaries

In this case, we assume that the boundary $x = b$ is considered as metallic (for instance, there is an incoming wave at the boundary $x = a$, travelling from the left to the right). A first-order Silver-Müller type absorbing condition is imposed at the boundary $x = a$. From the numerical point of view, this boundary condition is treated in a weak sense by using a flux decomposition inspired from the Steger-Warming[11] scheme classically used in the computational fluid dynamics context. However, such a flux decomposition requires the diagonalization of the jacobian matrix associated to a conservative formulation of eq. (6). In order to do so, we make use of :

$$\boldsymbol{Q} = \begin{pmatrix} D \\ B \end{pmatrix} = BW = \begin{pmatrix} \varepsilon & 0 \\ 0 & \mu \end{pmatrix} \begin{pmatrix} E \\ H \end{pmatrix}$$

Then, eq. (20) can be written as :

$$\frac{\partial \boldsymbol{Q}}{\partial t} + \frac{\partial G(\boldsymbol{Q})}{\partial x} = 0,\ G(\boldsymbol{Q}) = Z\boldsymbol{Q} \ \text{ with } \ Z \equiv Z(x) = \begin{pmatrix} 0 & -\dfrac{1}{\mu(x)} \\ -\dfrac{1}{\varepsilon(x)} & 0 \end{pmatrix} \tag{20}$$

The numerical flux which corresponds to the boundaries $x = a$ and $x = b$ is given by :

$$F_{\frac{1}{2}} = (-Z)_1^+ Q_1 + (-Z)_0^- Q_0,\ F_{\frac{1}{2}} = Z_N^+ Q_N + (Z)_{N+1}^- Q_{N+1}.$$

The matrix Z can be diagonalized as $Z = T\Lambda T^{-1}$ with :

$$\Lambda = \begin{pmatrix} -c & 0 \\ 0 & c \end{pmatrix} \quad , \quad T = \begin{pmatrix} 1 & 1 \\ c\mu & -c\mu \end{pmatrix} \quad \text{and} \quad T^{-1} = \frac{1}{2}\begin{pmatrix} 1 & c\varepsilon \\ 1 & -c\varepsilon \end{pmatrix}$$

We now compute its negative and positive parts :

$$Z^{\pm} = T\Lambda^{\pm}T^{-1},\ Z^+ = \frac{1}{2}\begin{pmatrix} c & -\dfrac{1}{\mu} \\ -\dfrac{1}{\varepsilon} & c \end{pmatrix} \quad , \quad Z^- = \frac{1}{2}\begin{pmatrix} -c & -\dfrac{1}{\mu} \\ -\dfrac{1}{\varepsilon} & -c \end{pmatrix}$$

The computation of the numerical flux $F_{\frac{1}{2}}$ requires the ghost state Q_0. Assume that we set $(-Z)_0^- Q_0 = 0$ then :

$$F_{\frac{1}{2}} = (-Z)_1^+ Q_1$$

Now the total flux for $j = 1$ is :

$$\Phi_{1,2} + \Phi_{1,0} = \frac{1}{2}(AW_2 + AW_1) + (-Z)_1^+ B_1 W_1 = -\frac{1}{2}\begin{pmatrix} H_2 - c_1\varepsilon_1 E_1 \\ E_2 - c_1\mu_1 H_1 \end{pmatrix} \tag{21}$$

By using eq. (21) in the context of the Crank-Nicolson scheme for $j = 1$, eq. (13) are modified as follows :

$$\left\{ \begin{array}{lcl} \varepsilon_1(\sigma_1 + c_1)E_1^{n+1} - H_2^{n+1} & = & \varepsilon_1(\sigma_1 - c_1)E_1^n + H_2^n \\ \mu_1(\sigma_1 + c_1)H_1^{n+1} - E_2^{n+1} & = & \mu_1(\sigma_1 - c_1)H_1^n + E_2^n \end{array} \right. \tag{22}$$

For the metallic boundary at $j = N$ we proceed as in subsection 2.3.1. In summary, the first and the last diagonal 2×2 blocks of M and P must be modified as :

$$\left\{ \begin{array}{lcl} M_{11} & = & \sigma_1 B_1 + D_1 \\ M_{NN} & = & \sigma_N B_N - C_N \end{array} \right. \quad \left\{ \begin{array}{lcl} P_{11} & = & \sigma_1 B_1 - D_1 \\ P_{NN} & = & \sigma_N B_N + C_N \end{array} \right. \tag{23}$$

where :

$$D_1 = \begin{pmatrix} c_1\varepsilon_1 & 0 \\ 0 & c_1\mu_1 \end{pmatrix}$$

2.4 Theoretical aspects

In this section we study some of the mathematical properties of the Implicit Finite Volume Time Domain (IFVTD) method proposed previously. The following aspects are considered : conservation of a discrete form of the electromagnetic energy, inversibility of the implicit matrix chracterizing the IFVTD method and evaluation of the numerical dispersion.

2.4.1 Energetic considerations

We recall that, in the general (3D) continuous, isotropic case, the electromagnetic energy verifies some conservation equation (Poynting's theorem) for the Maxwell's equations with no current. This theorem states that :

$$\frac{d}{dt}\left(\int_V \mathcal{E} dv\right) + \int_{\partial V} \mathcal{P} \cdot \mathbf{n} ds = 0 \tag{24}$$

for any closed volume V with a regular boundary ∂V, where the electromagnetic energy $\mathcal{E}$ and the Poynting's vector $\mathbf{P}$ are respectively given by :

$$\mathcal{E} = \frac{1}{2}\left[\varepsilon\, {}^t\boldsymbol{E}\boldsymbol{E} + \mu\, {}^t\boldsymbol{H}\boldsymbol{H}\right] \quad , \quad \mathcal{P} = \mathbf{E} \times \mathbf{H}$$

In the three-dimensional case, $\boldsymbol{E}$ and $\boldsymbol{H}$ are vectors whose elements are the x, y and z components of the electric and magnetic fields. Note that for a given metallic boundary, $\mathbf{E} \times \mathbf{n} = 0$ and Poynting's theorem yields that the electromagnetic energy is exactly conserved. In this section, we study the behaviour of the electromagnetic energy in the discrete case when the time evolution of the electromagnetic field is given by the implicit scheme (12).

Proposition 1 *The discret electromagnetic energy given by :*

$$\mathcal{E}^n = \frac{1}{2}\sum_{j=1}^{N} \Delta x_j \left[\varepsilon_j (E_j^n)^2 + \mu_j (H_j^n)^2\right] \tag{25}$$

is decreasing in time, that is $\mathcal{E}^{n+1} \leq \mathcal{E}^n$. If the computational domain doesn't posses absorbing boundaries, this energy remains constant.

Proof If we multiply the first equation of (12) by $\frac{E_j^{n+1}+E_j^n}{2}\Delta x_j$ and the second one by $\frac{H_j^{n+1}+H_j^n}{2}\Delta x_j$, then add the results, re-arrange the terms and sum over all j we get :

$$\frac{\mathcal{E}^{n+1}-\mathcal{E}^n}{\Delta t} = \sum_{j=1}^{N} (\mathcal{P}_{j+\frac{1}{2}}^{n+\frac{1}{2}} - \mathcal{P}_{j-\frac{1}{2}}^{n+\frac{1}{2}}) \tag{26}$$

where $\mathcal{P}_{j+\frac{1}{2}}^{n+\frac{1}{2}}$ is defined by :

$$\mathcal{P}_{j+\frac{1}{2}}^{n+\frac{1}{2}} = \frac{1}{2}\left[\frac{E_j^{n+1}+E_j^n}{2}\cdot\frac{H_{j+1}^{n+1}+H_{j+1}^n}{2} + \frac{E_{j+1}^{n+1}+E_{j+1}^n}{2}\cdot\frac{H_j^{n+1}+H_j^n}{2}\right]$$

$\mathcal{P}_{j+\frac{1}{2}}^{n+\frac{1}{2}}$ can be seen as a discrete counterpart of the Poynting vector and the equation (26) the discrete form of the Poynting equation (24). Eq. (26) can be simplified to yield :

$$\frac{\mathcal{E}^{n+1}-\mathcal{E}^n}{\Delta t} = \mathcal{P}_{N+\frac{1}{2}}^{n+\frac{1}{2}} - \mathcal{P}_{\frac{1}{2}}^{n+\frac{1}{2}} \tag{27}$$

At this point, we must take into account the three configurations of boundary conditions as considered in subsections 2.3.1 to 2.3.3.

Metallic boundaries. We obtain :

$$\begin{cases} \mathcal{P}_{\frac{1}{2}}^{n+\frac{1}{2}} = \frac{1}{2}\left[\frac{-(E_1^{n+1}+E_1^n)}{2}\cdot\frac{H_1^{n+1}+H_1^n}{2} + \frac{E_1^{n+1}+E_1^n}{2}\cdot\frac{H_1^{n+1}+H_1^n}{2}\right] = 0 \\ \mathcal{P}_{N+\frac{1}{2}}^{n+\frac{1}{2}} = \frac{1}{2}\left[\frac{E_N^{n+1}+E_N^n}{2}\cdot\frac{H_N^{n+1}+H_N^n}{2} + \frac{-(E_N^{n+1}+E_N^n)}{2}\cdot\frac{H_N^{n+1}+H_N^n}{2}\right] = 0 \end{cases}$$

and thus $\mathcal{E}^{n+1} = \mathcal{E}^n$.

Periodic boundaries. We obtain :

$$\begin{cases} \mathcal{P}_{\frac{1}{2}}^{n+\frac{1}{2}} = \frac{1}{2}\left[\frac{E_N^{n+1}+E_N^n}{2}\cdot\frac{H_1^{n+1}+H_1^n}{2} + \frac{E_1^{n+1}+E_N^n}{2}\cdot\frac{H_1^{n+1}+H_N^n}{2}\right] \\ \mathcal{P}_{N+\frac{1}{2}}^{n+\frac{1}{2}} = \frac{1}{2}\left[\frac{E_N^{n+1}+E_N^n}{2}\cdot\frac{H_1^{n+1}+H_1^n}{2} + \frac{E_1^{n+1}+E_1^n}{2}\cdot\frac{H_N^{n+1}+H_N^n}{2}\right] \end{cases}$$

that is $\mathcal{P}_{\frac{1}{2}}^{n+\frac{1}{2}} = \mathcal{P}_{N+\frac{1}{2}}^{n+\frac{1}{2}}$ and thus $\mathcal{E}^{n+1} = \mathcal{E}^n$.

Metallic and absorbing boundaries. Taking into account eq. (22) for $j = 1$, it is easily shown that :

$$\frac{\mathcal{E}^{n+1} - \mathcal{E}^n}{\Delta t} = \mathcal{P}_{N+\frac{1}{2}}^{n+\frac{1}{2}} - \mathcal{P}_{\frac{1}{2}}^{n+\frac{1}{2}}$$

with :

$$\begin{cases} \mathcal{P}_{\frac{1}{2}}^{n+\frac{1}{2}} = \dfrac{1}{2}\left[\dfrac{c_1\varepsilon_1}{4}(E_1^{n+1} + E_1^n)^2 + \dfrac{c_1\mu_1}{4}(H_1^{n+1} + H_1^n)^2\right] \geq 0 \\ \mathcal{P}_{N+\frac{1}{2}}^{n+\frac{1}{2}} = \dfrac{1}{2}\left[\dfrac{E_N^{n+1} + E_N^n}{2} \cdot \dfrac{H_N^{n+1} + H_N^n}{2} + \dfrac{-(E_N^{n+1} + E_N^n)}{2} \cdot \dfrac{H_N^{n+1} + H_N^n}{2}\right] = 0 \end{cases}$$

and thus $\mathcal{E}^{n+1} \leq \mathcal{E}^n$.

■

2.4.2 Inversibility of the implicit matrix

Taking into account the three configurations of boundary conditions, the matrix M of eq. (15) and (16) can be decomposed as :

$$M = D_m + M_m \tag{28}$$

where D_m is a block-diagonal matrix and M_m is a skew-symmetric matrix.

Metallic boundaries. We have :

$$D_m = \text{diag}\,(\sigma_1 B_1 + C_1\ ,\ \sigma_2 B_2\ ,\ \cdots\ ,\ \sigma_{N-1} B_{N-1}\ ,\ \sigma_N B_N - C_N)$$

Periodic boundaries. We have :

$$D_m = \text{diag}\,(\sigma_1 B_1\ ,\ \sigma_2 B_2\ ,\ \cdots\ ,\ \sigma_{N-1} B_{N-1}\ ,\ \sigma_N B_N)$$

Metallic and absorbing boundaries. We have :

$$D_m = \text{diag}\,(\sigma_1 B_1 + D_1\ ,\ \sigma_2 B_2\ ,\ \cdots\ ,\ \sigma_{N-1} B_{N-1}\ ,\ \sigma_N B_N - C_N)$$

Proposition 2 *The implicit matrix given by the relations (15) and (16) is positive definite and therefore invertible.*

Proof Since for each of the above configurations the matrix M_m is skew-symmetric we have that for any $\mathbf{X} \in \mathbb{R}^{2N}$:

$$\mathbf{X}^t M \mathbf{X} = \mathbf{X}^t D_m \mathbf{X}$$

Each case of boundary condition is now considered separately.

Metallic boundaries. Since C_1 and C_N are both skew-symmetric matrices we obtain for $X \neq 0$:

$$\mathbf{X}^t D_m \mathbf{X} = \sum_{i=1}^{N} X_i^t \sigma_i B_i X_i > 0$$

and M is positive definite and thus invertible.

Periodic boundaries. We obtain for $X \neq 0$:

$$\mathbf{X}^t D_m \mathbf{X} = \sum_{i=1}^{N} X_i^t \sigma_i B_i X_i > 0$$

and M is positive definite and thus invertible.

Metallic and absorbing boundaries. We obtain for $X \neq 0$:

$$\mathbf{X}^t D_m \mathbf{X} = X_1^t (\sigma_1 B_1 + D_1) X_1 + \sum_{i=2}^{N} X_i^t \sigma_i B_i X_i > 0$$

and M is positive definite and thus invertible.

■

2.4.3 Study of the numerical dispersion

The implicit scheme (12) for $\varepsilon_j = \varepsilon$, $\mu_j = \mu$, $\forall j$ (constant ε and μ in the whole domain) and for a uniform mesh $\Delta x_j = \Delta x$ writes :

$$\left\{ \begin{array}{rcl} \dfrac{E_j^{n+1} - E_j^n}{\Delta t} & = & \dfrac{1}{4\varepsilon \Delta x} \left[(H_{j+1}^n + H_{j+1}^{n+1}) - (H_{j-1}^n + H_{j-1}^{n+1}) \right] \\ \dfrac{H_j^{n+1} - H_j^n}{\Delta t} & = & \dfrac{1}{4\mu \Delta x} \left[(E_{j+1}^n + E_{j+1}^{n+1}) - (E_{j-1}^n + E_{j-1}^{n+1}) \right] \end{array} \right. \tag{29}$$

Eq. (29) can also be written as the discretization of a second-order wave type equation for E. For this purpose, we first deduce from the first relation of eq. (29) :

$$\begin{array}{rcl} \dfrac{E_j^{n+2} - 2E_j^{n+1} + E_j^n}{(\Delta t)^2} & = & \dfrac{1}{\Delta t} \left(\dfrac{E_j^{n+2} - E_j^{n+2}}{\Delta t} - \dfrac{E_j^{n+1} - E_j^n}{\Delta t} \right) \\ & = & \dfrac{1}{4\varepsilon \Delta x} \left[\dfrac{H_{j+1}^{n+2} - H_{j+1}^{n+1}}{\Delta t} + \dfrac{H_{j+1}^{n+1} - H_{j+1}^n}{\Delta t} - \right. \\ & & \left. \dfrac{H_{j-1}^{n+2} - H_{j-1}^{n+1}}{\Delta t} - \dfrac{H_{j-1}^{n+1} - H_{j-1}^n}{\Delta t} \right] \end{array}$$

then, by using the second relation we get :

$$\begin{aligned}\frac{E_j^{n+2}-2E_j^{n+1}+E_j^n}{(\Delta t)^2} &= \frac{c^2}{4}\left[\frac{(E_{j+2}^{n+2}-2E_j^{n+2}+E_{j-2}^{n+2})}{4(\Delta x)^2}+2\frac{(E_{j+2}^{n+1}-2E_j^{n+1}+E_{j-2}^{n+1})}{4(\Delta x)^2}\right] \\ &+ \frac{c^2}{4}\left[\frac{(E_{j+2}^{n}-2E_j^{n}+E_{j-2}^{n})}{4(\Delta x)^2}\right]\end{aligned} \tag{30}$$

which is a consistent approximation of the wave equation for E. By doing a similar manipulation for the explicit scheme we get the following consistent approximation of the wave equation :

$$\frac{H_j^{n+1}-2H_j^n+H_j^{n-1}}{(\Delta t)^2}=\frac{c^2}{4}\frac{H_{j+2}^n-2H_j^n+H_{j-2}^n}{(\Delta x)^2} \tag{31}$$

Numerical dispersion for the implicit scheme. If we introduce in the numerical scheme (30) an harmonic wave $E_j^n = E_0 e^{i(kj\Delta x-\omega_d n\Delta t)}$ we get :

$$\frac{(e^{i\omega_d\Delta t}-1)^2}{(\Delta t)^2}=\frac{c^2}{16(\Delta x)^2}(e^{i\omega_d\Delta t}+1)^2(e^{2ik\Delta x}+e^{-2ik\Delta x}-2)$$

that can be simplified as :

$$\frac{\sin^2\left(\frac{\omega_d\Delta t}{2}\right)}{(\Delta t)^2}=\frac{c^2}{4}\cos^2\left(\frac{\omega_d\Delta t}{2}\right)\frac{\sin^2(k\Delta x)}{(\Delta x)^2}$$

from which we can deduce an expression for the ratio of the numerical pulsation ω_d to the exact pulsation kc as a function of Δx and the CFL number $\alpha=\dfrac{c\Delta t}{\Delta x}$:

$$\begin{aligned}\frac{\omega_d}{kc} &= \pm\frac{2}{kc\Delta t}\arctan\left(\frac{c\Delta t}{2\Delta x}\sin(k\Delta x)\right) \\ &= \pm\frac{2}{\alpha k\Delta x}\arctan\left(\frac{\alpha}{2}\sin(k\Delta x)\right)\end{aligned}$$

Clearly, the above ratio yields a criterion for evaluating the numerical dispersion of the overall scheme. If we denote by $K=k\Delta x$ and using Taylor expansions of the terms involved we obtain :

$$q_{\text{imp}}(\alpha,K)=\frac{\omega_d}{kc}=1-\frac{\alpha^2+2}{12}K^2+\frac{2+10\alpha^2+3\alpha^4}{240}K^4+\mathcal{O}(K^5) \tag{32}$$

The behaviour of the quantity $q_{\text{imp}}(\alpha,K)$ is represented on figure 2 for different values of the CFL number α, as a function of K. We can see that :

- for a fixed α, q_{imp} is a decreasing function of K.
- for a fixed K, q_{imp} is a decreasing function of α (as the CFL number increases the dispersion properties get worse).

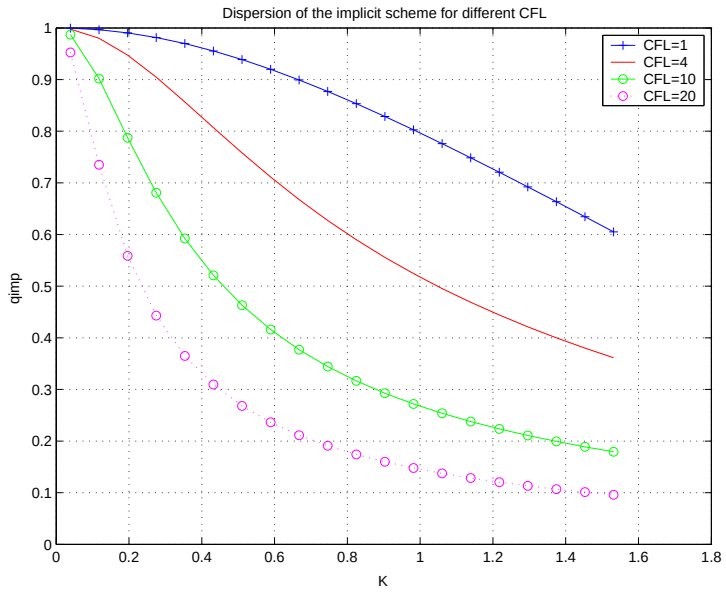

FIG. 2 – Numerical dispersion of the implicit scheme for different values of the CFL number

Numerical dispersion for the explicit scheme. If we introduce in the numerical scheme (31) an harmonic wave $H_j^n = H_0 e^{i(kj\Delta x - \omega_d n \Delta t)}$ we get :

$$\frac{e^{i\omega\Delta t} + e^{-i\omega\Delta t} - 2}{(\Delta t)^2} = \frac{c^2}{4(\Delta x)^2}(e^{2ik\Delta x} + e^{-2ik\Delta x} - 2)$$

that can be simplified as :

$$\frac{\sin^2\left(\dfrac{\omega_d \Delta t}{2}\right)}{(\Delta t)^2} = \frac{c^2}{4}\frac{\sin^2(k\Delta x)}{(\Delta x)^2}$$

from which we obtain :

$$\begin{aligned}\frac{\omega_d}{kc} &= \pm\frac{2}{kc\Delta t}\arcsin\left(\frac{c\Delta t}{2\Delta x}\sin(k\Delta x)\right)\\ &= \pm\frac{2}{\alpha k\Delta x}\arcsin\left(\frac{\alpha}{2}\sin(k\Delta x)\right)\end{aligned}$$

If we denote by $K = k\Delta x$ and using Taylor expansions of the terms involved we obtain :

$$q_{\text{exp}}(\alpha, K) = \frac{\omega_d}{kc} = 1 + \frac{\alpha^2 - 4}{24}K^2 + \frac{(\alpha-2)^2(3\alpha-2)^2}{1920}K^4 + \mathcal{O}(K^5) \tag{33}$$

The behaviour of the quantity $q_{\text{exp}}(\alpha, K)$ is shown on figure 3. We note that for a fixed α, q_{exp} is a decreasing function of K and for a fixed K, q_{exp} is an increasing function of α (which means that we can take the maximum α allowed by the stability condition to improve the dispersion properties).

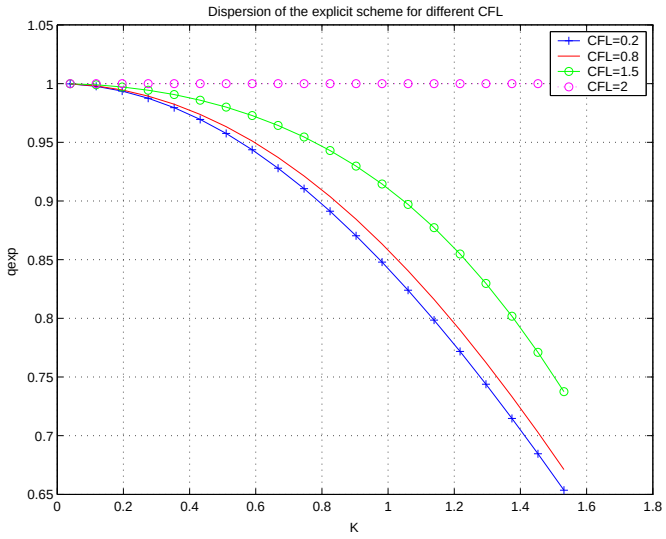

FIG. 3 – Numerical dispersion of the explicit scheme for different values of the CFL number

Remark 1 *From the previous expressions we can make the following remarks :*

- *the implicit scheme is second-order accurate for every value of α but the explicit scheme is at least of order 5 if $\alpha = 2$ (for the 1D ideal situation). This value is the maximum value for which the explicit scheme is stable.*
- *for a fixed α and as $K \to 0$ we have that $q_{imp}(\alpha, K) < q_{exp}(\alpha, K)$ therefore the implicit scheme is more dispersive than the explicit one (as seen in [8]).*

The expressions (32) and (33) can be re-written as :

$$\begin{cases} q_{\text{imp}} &= \dfrac{2}{\bar{\omega}} \arctan\left(\dfrac{\bar{\omega}}{2K}\sin K\right) \\ q_{\text{exp}} &= \dfrac{2}{\bar{\omega}} \arcsin\left(\dfrac{\bar{\omega}}{2K}\sin K\right) \end{cases}$$

where $\bar{\omega} = \omega\Delta t = kc\Delta t = 2\pi n$ with $n = \dfrac{T}{\Delta t}$ is the number of time discretization points per period. If we take into account the fact that $K \in [0, \pi]$, in order to preserve the stability of the explicit scheme we need to impose in this case $K \geq K_{\min} = \dfrac{\bar{\omega}}{2}$, which means that we cannot choose an arbitrarly small space discretization step which is not the case if we use the implicit scheme. In order to better illustrate this property we choose for example $\bar{\omega} \in \left[\dfrac{2\pi}{30}, \dfrac{2\pi}{3}\right]$, that is we use between 3 and 30 time discretization points per period. The corresponding behaviours of q_{imp} and q_{exp} are shown on figure 4.

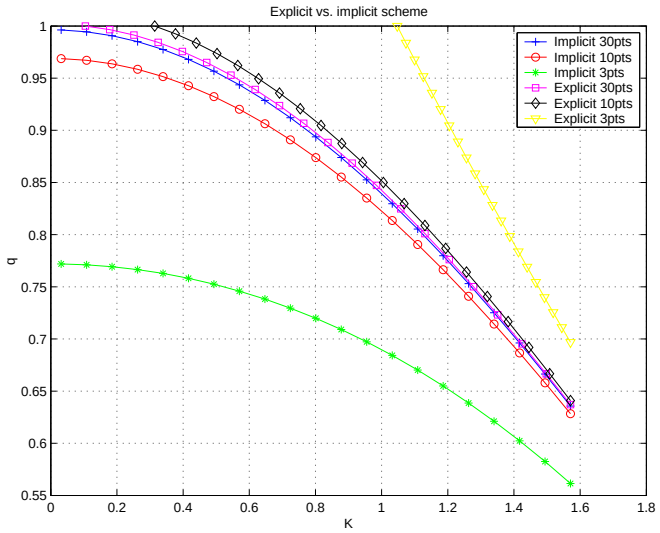

FIG. 4 – Numerical dispersion of the explicit and implicit schemes for different values of $\bar{\omega}$

2.5 Numerical results

We present here numerical results from the resolution of the 1D Maxwell equations using the explicit and implicit finite volume time domain methods studied previously. The problem under consideration is given by the propagation of a pulse in the domain $[0, 1]$. The pulse is initiated at the position $x = 0.15$ and propagates from the left to right.

Test case 1 : homogeneous domain ($\varepsilon(x) = \varepsilon_0 \quad \forall x \in [0, 1]$), using a uniform mesh with $N = 200$ points and a $CFL = 2$ (the explicit scheme is exact). The solution is shown on figure 5 after $n = 60$ time steps (before reflection) and and after $n = 120$ time steps (after reflection). As expected, in this ideal situation for the explicit scheme, the implicit scheme is more dispersive than the explicit one.

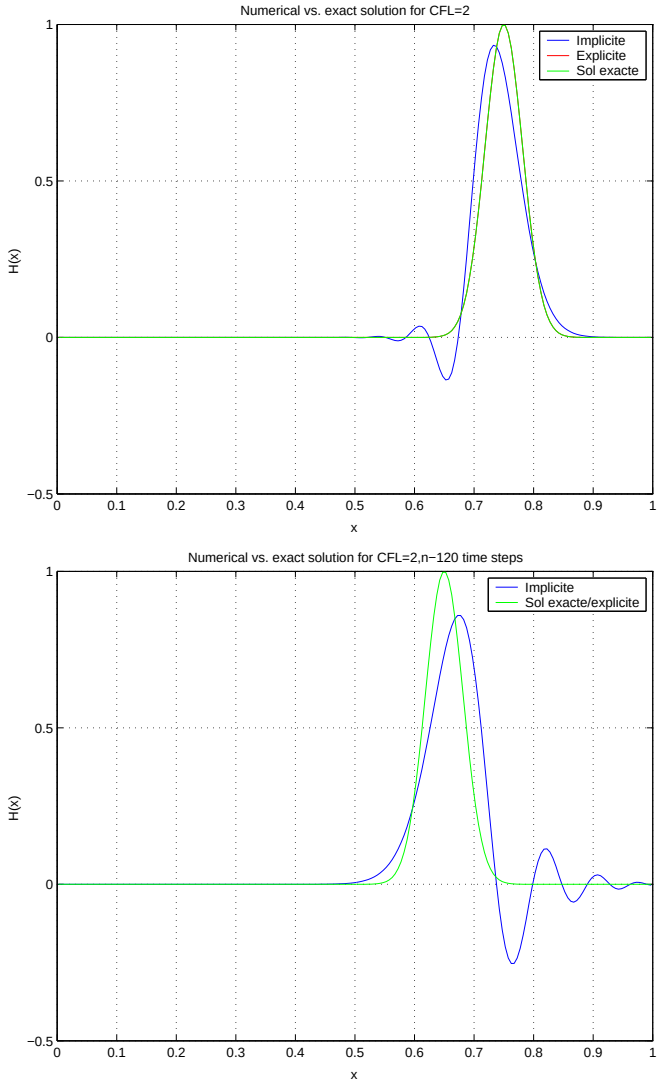

FIG. 5 – Test case 1 : homogeneous domain, uniform mesh

Test case 2 : similar to **test case 1** but with a non-uniform mesh (random mesh size generated by a uniform law, such that $\Delta x_i \in [0.0025, 0.0075]$) still with $N = 200$ points. The solution is shown on figure 6 after $n = 100$ time steps (before reflection) and and after $n = 200$ time steps (after reflection). We can see that in the non-uniform case the dispersion of the two schemes is of the same order.

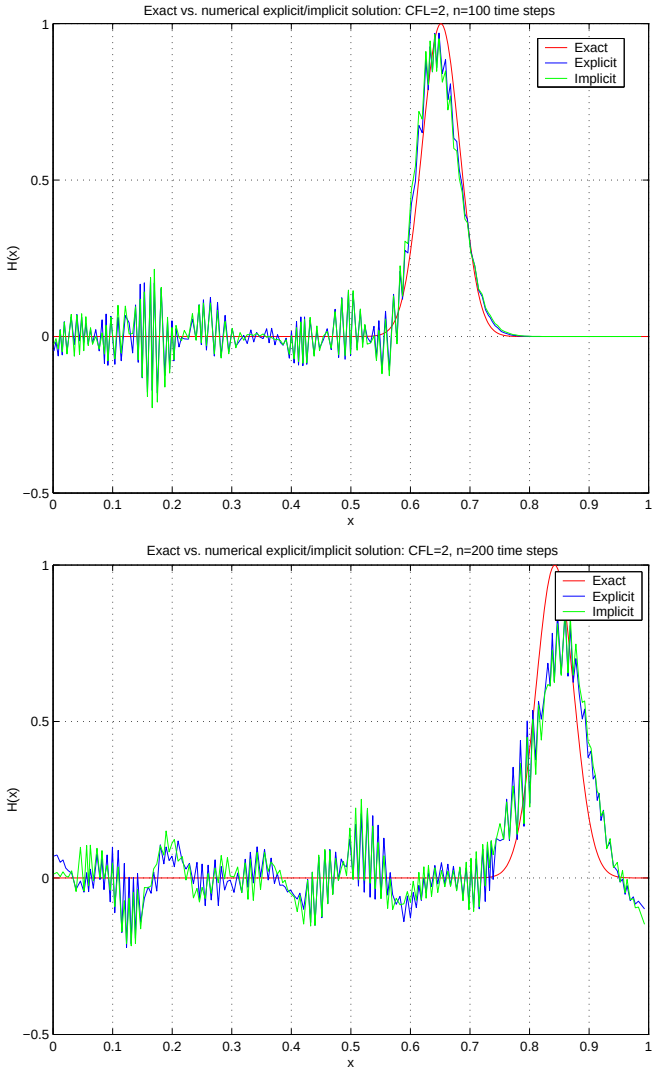

FIG. 6 – Test case 2 : homogeneous domain, nonuniform mesh

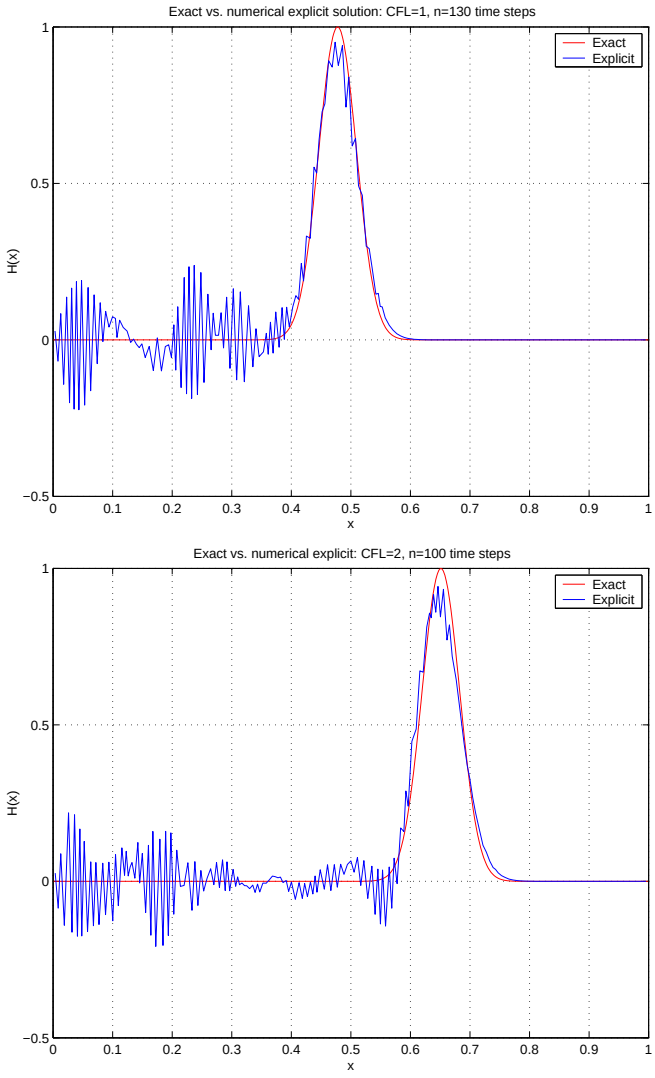

FIG. 7 – Explicit scheme for different CFL : CFL=1, CFL=2

For the same mesh we can also compare the properties of the explicit scheme for different values of the CFL number. On figure 7, one can see that we cannot get any conclusion on the dispersive nature of the explicit scheme as the CFL number gets closer to its maximum allowed value.

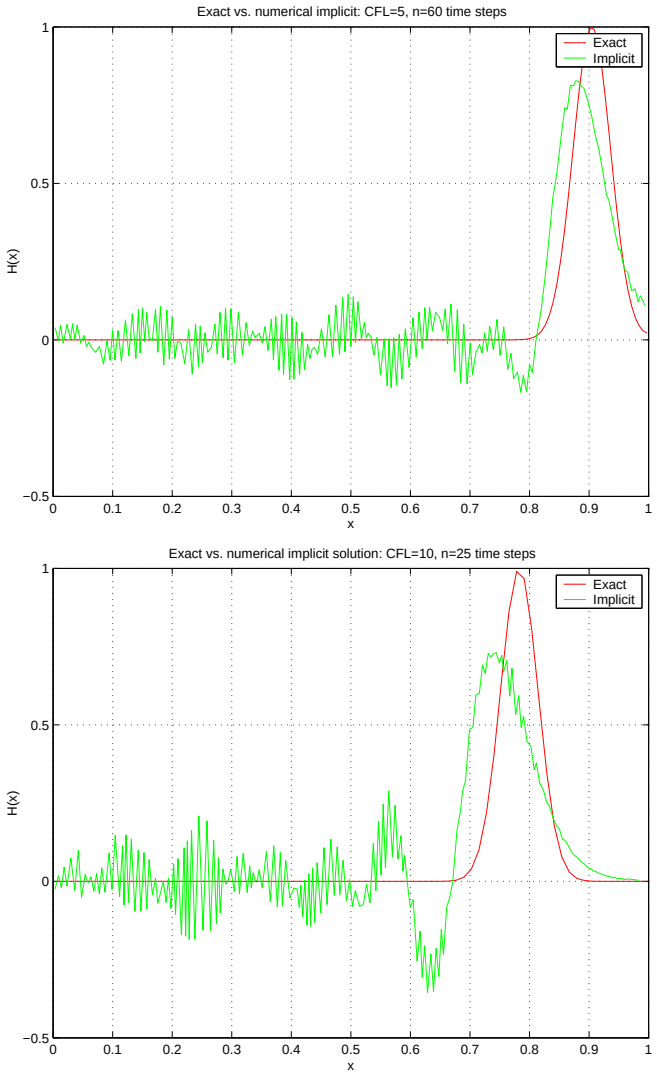

FIG. 8 – Implicit scheme for different CFL : CFL=5, CFL=10

As the implicit scheme is always stable, larger values of the CFL numbers are allowed. On figure 8, the behaviour for $CFL = 5$ and $CFL = 10$ are shown.

3 3D Maxwell equations

We consider now the three dimensional Maxwell equations (1 that we rewrite as :

$$\left\{ \begin{array}{rcl} \varepsilon(\boldsymbol{x})\dfrac{\partial \boldsymbol{E}}{\partial t} + N_x\dfrac{\partial \boldsymbol{H}}{\partial x} + N_y\dfrac{\partial \boldsymbol{H}}{\partial y} + N_z\dfrac{\partial \boldsymbol{H}}{\partial z} & = & 0 \\ \mu(\boldsymbol{x})\dfrac{\partial \boldsymbol{H}}{\partial t} - N_x\dfrac{\partial \boldsymbol{E}}{\partial x} - N_y\dfrac{\partial \boldsymbol{E}}{\partial y} - N_z\dfrac{\partial \boldsymbol{E}}{\partial z} & = & 0 \end{array} \right. \tag{34}$$

where :

$$\boldsymbol{E} = \begin{pmatrix} E_x \\ E_y \\ E_z \end{pmatrix} \quad \text{and} \quad \boldsymbol{H} = \begin{pmatrix} H_x \\ H_y \\ H_z \end{pmatrix}$$

The matrices N_x, N_y and N_z are given by :

$$N_x = \begin{pmatrix} 0 & 0 & 0 \\ 0 & 0 & 1 \\ 0 & -1 & 0 \end{pmatrix} \quad N_y = \begin{pmatrix} 0 & 0 & -1 \\ 0 & 0 & 0 \\ 1 & 0 & 0 \end{pmatrix} \quad N_z = \begin{pmatrix} 0 & 1 & 0 \\ -1 & 0 & 0 \\ 0 & 0 & 0 \end{pmatrix} \tag{35}$$

Note that for any vector X and for any $\mathbf{n} = (n_x, n_y, n_z)^t$ the matrix $N_{\mathbf{n}} = n_x N_x + n_y N_y + n_z N_z$ is skew-symetric and $N_{\mathbf{n}}\mathbf{u} = \mathbf{u} \times \mathbf{n}$. System (35) is solved on a bounded domain Ω with boundary $\partial\Omega = \partial\Omega_m \cup \partial\Omega_\infty$. We impose on the border of the domain two types of boundary conditions : a metallic boundary condition on $\partial\Omega_m$ (i.e $\mathbf{n} \times \boldsymbol{E} = 0$) and a Silver-Müller boundary condition on $\partial\Omega_\infty$ (i.e $\mathbf{n} \times \boldsymbol{E} + c(\boldsymbol{x})\mu(\boldsymbol{x})\mathbf{n} \times (\mathbf{n} \times \boldsymbol{H}) = 0$). The Maxwell eqauations (34) can also be written in conservative form as :

$$Q\boldsymbol{W}_t + \nabla.F(\boldsymbol{W}) = 0 \tag{36}$$

with :

$$Q = \begin{pmatrix} \varepsilon(\mathbf{x})I_3 & 0_3 \\ 0_3 & \mu(\mathbf{x})I_3 \end{pmatrix} \quad , \quad \boldsymbol{W} = \begin{pmatrix} E_x \\ E_y \\ E_z \\ H_x \\ H_y \\ H_z \end{pmatrix} \quad \text{et} \quad F(\boldsymbol{W}) = \begin{pmatrix} F^x(\boldsymbol{W}) \\ F^y(\boldsymbol{W}) \\ F^x z(\boldsymbol{W}) \end{pmatrix}$$

$F(\boldsymbol{W})$ being defined in the following way :

$$F^{x_1}(\boldsymbol{W}) = \begin{pmatrix} 0 \\ H_z \\ -H_y \\ 0 \\ -E_z \\ E_y \end{pmatrix} \quad , \quad F^{x_2}(\boldsymbol{W}) = \begin{pmatrix} -H_z \\ 0 \\ H_x \\ E_z \\ 0 \\ -E_x \end{pmatrix} \quad \text{and} \quad F^{x_3}(\boldsymbol{W}) = \begin{pmatrix} H_y \\ -H_x \\ 0 \\ -E_y \\ E_x \\ 0 \end{pmatrix}$$

Before proceeding with the finite volume formulation we recall that the following matrix :

$$Z_{\mathbf{n}} = \begin{pmatrix} \mathrm{O}_3 & -N_{\mathbf{n}} \\ N_{\mathbf{n}} & \mathrm{O}_3 \end{pmatrix}$$

can be decomposed in positive and negative parts as follows :

$$\left\{ \begin{array}{rcl} Z_{\mathbf{n}}^{+} & = & \dfrac{c(\boldsymbol{x})}{2} \begin{pmatrix} -N_{\mathbf{n}}^2 & \bar{z}(\boldsymbol{x})N_{\mathbf{n}} \\ -z(\boldsymbol{x})N_{\mathbf{n}} & -N_{\mathbf{n}}^2 \end{pmatrix} \\ Z_{\mathbf{n}}^{-} & = & \dfrac{c(\boldsymbol{x})}{2} \begin{pmatrix} N_{\mathbf{n}}^2 & \bar{z}(\boldsymbol{x})N_{\mathbf{n}} \\ -z(\boldsymbol{x})N_{\mathbf{n}} & N_{\mathbf{n}}^2 \end{pmatrix} \end{array} \right. \tag{37}$$

A general flux decomposition based on $Z_{\mathbf{n}}^{\pm}$ writes as :

$$\Phi_{\pm}(\boldsymbol{Q}_l, \boldsymbol{Q}_r, \mathbf{n}_{lr}) = (Z_{\mathbf{n}}^{+})_l \boldsymbol{Q}_l + (Z_{\mathbf{n}}^{-})_r \boldsymbol{Q}_r \tag{38}$$

or, equivalently :

$$\Phi_{\pm}(\boldsymbol{W}_l, \boldsymbol{W}_r, \mathbf{n}_{lr}) = (Z_{\mathbf{n}}^{+})_l (D_w)_l \boldsymbol{W}_l + (Z_{\mathbf{n}}^{-})_r (D_w)_r \boldsymbol{W}_r \tag{39}$$

where :

$$D_w = \begin{pmatrix} \varepsilon(\boldsymbol{x})\mathrm{I}_3 & \mathrm{O}_3 \\ \mathrm{O}_3 & \mu(\boldsymbol{x})\mathrm{I}_3 \end{pmatrix}$$

Note that $N_{\mathbf{n}}^3 = -N_{\mathbf{n}}$ and then, $\forall\ \boldsymbol{W}$, we have :

$$\begin{array}{rcl} Z_{\mathbf{n}}^{-} D_w \boldsymbol{W} & = & \dfrac{c(\boldsymbol{x})}{2} \begin{pmatrix} N_{\mathbf{n}}^2 & -\bar{z}(\boldsymbol{x})N_{\mathbf{n}}^3 \\ -z(\boldsymbol{x})N_{\mathbf{n}} & N_{\mathbf{n}}^2 \end{pmatrix} \begin{pmatrix} \varepsilon(\boldsymbol{x})\mathrm{I}_3 & \mathrm{O}_3 \\ \mathrm{O}_3 & \mu(\boldsymbol{x})\mathrm{I}_3 \end{pmatrix} \begin{pmatrix} \boldsymbol{E} \\ \boldsymbol{H} \end{pmatrix} \\ & = & \dfrac{c(\boldsymbol{x})}{2} \begin{pmatrix} N_{\mathbf{n}} & \mathrm{O}_3 \\ \mathrm{O}_3 & z(\boldsymbol{x})\mathrm{I}_3 \end{pmatrix} \begin{pmatrix} N_{\mathbf{n}} & -\bar{z}(\boldsymbol{x})N_{\mathbf{n}}^2 \\ -N_{\mathbf{n}} & \bar{z}(\boldsymbol{x})N_{\mathbf{n}}^2 \end{pmatrix} \begin{pmatrix} \varepsilon(\boldsymbol{x})\boldsymbol{E} \\ \mu(\boldsymbol{x})\boldsymbol{H} \end{pmatrix} \\ & = & \dfrac{c(\boldsymbol{x})}{2} \begin{pmatrix} N_{\mathbf{n}} & \mathrm{O}_3 \\ \mathrm{O}_3 & z(\boldsymbol{x})\mathrm{I}_3 \end{pmatrix} \begin{pmatrix} \varepsilon(\boldsymbol{x})N_{\mathbf{n}}\boldsymbol{E} - \bar{z}(\boldsymbol{x})\mu(\boldsymbol{x})N_{\mathbf{n}}^2\boldsymbol{H} \\ -\varepsilon(\boldsymbol{x})N_{\mathbf{n}}\boldsymbol{E} + \bar{z}(\boldsymbol{x})\mu(\boldsymbol{x})N_{\mathbf{n}}^2\boldsymbol{H} \end{pmatrix} \end{array}$$

Morevover :

$$\begin{array}{rcl} \mathbf{n} \times \boldsymbol{E} + c(\boldsymbol{x})\mu(\boldsymbol{x})\mathbf{n} \times (\mathbf{n} \times \boldsymbol{H}) & = & -N_{\mathbf{n}}\boldsymbol{E} + c(\boldsymbol{x})\mu(\boldsymbol{x})N_{\mathbf{n}}^2\boldsymbol{H} \\ & = & \dfrac{1}{\varepsilon(\boldsymbol{x})}\left(-\varepsilon(\boldsymbol{x})N_{\mathbf{n}}\boldsymbol{E} + c(\boldsymbol{x})\varepsilon(\boldsymbol{x})\mu(\boldsymbol{x})N_{\mathbf{n}}^2\boldsymbol{H}\right) \\ & = & \dfrac{1}{\varepsilon(\boldsymbol{x})}\left(-\varepsilon(\boldsymbol{x})N_{\mathbf{n}}\boldsymbol{E} + \bar{z}(\boldsymbol{x})\mu(\boldsymbol{x})N_{\mathbf{n}}^2\boldsymbol{H}\right) \end{array}$$

Thus, the Silver-Müller boundary condition whihs is imposed on the $\partial\Omega_\infty$ can be taken into account by setting :

$$(Z_{\mathbf{n}}^{-} D_w \boldsymbol{W})_\infty = 0$$

3.1 Finite volume discretization

The domain Ω is discretized using control volumes (or cell) C_i where C_i is here taken to be a thetrahedorn of the mesh. On each cell C_i we denote by $\mathbf{n}_{ij}$ the outwards normal vector on the interface between two neighboring cells C_i and C_j (i.e the triangular face shared by two neighboring tetrahedra), directed from C_i to C_j,and $N_{ij} = N_{n_{ij}}$ i.e the operator $. \times \mathbf{n}_{ij}$ (note that in the present case $\mathbf{n}_{ij}$ is not a unitary vector). We define the mean value of W on C_i denoted by W_i as :

$$W_i = \frac{1}{V_i} \int_{C_i} W(x,t) dx$$

where W is any component of $\boldsymbol{E}$ or $\boldsymbol{H}$ and $V_i = \text{vol}(C_i)$ is the volume of the cell C_i. A weak formulation of the problem under consideration is obtained by multiplying the equations by a test function φ_i and integrating over each cell we get :

$$\begin{aligned} &\int_{C_i} \varphi_i \left(Q\boldsymbol{W}_t + \nabla . F(\boldsymbol{W}) \right) d\omega = 0 \\ &\int_{C_i} \varphi_i Q\boldsymbol{W}_t d\omega + \int_{C_i} \varphi_i \left(\nabla . F(\boldsymbol{W}) \right) d\omega = 0 \end{aligned} \tag{40}$$

Now, choosing φ_i as the characteristic function associated to the cell C_i and applying a Green integration rule we obtain :

$$\int_{C_i} \varphi_i Q\boldsymbol{W}_t d\omega + \int_{C_i} \varphi_i \left(\nabla . F(\boldsymbol{W}) \right) d\omega = 0 \Leftrightarrow \int_{C_i} Q\boldsymbol{W}_t d\omega + \int_{\partial C_i} \left(F(\boldsymbol{W}) . \mathbf{n} \right) d\sigma = 0 \tag{41}$$

or equivalently :

$$\left\{ \begin{array}{rcl} \varepsilon_i V_i \dfrac{d\boldsymbol{E}_i}{dt} + \displaystyle\int_{\partial C_i} N_{\mathbf{n}} \boldsymbol{H} ds & = & 0 \\ \mu_i V_i \dfrac{d\boldsymbol{H}_i}{dt} - \displaystyle\int_{\partial C_i} N_{\mathbf{n}} \boldsymbol{E} ds & = & 0 \end{array} \right. \tag{42}$$

In the above expressions ε_i and μ_i are constant values on the tetrahedron C_i. In the present case ∂C_i is formed of the four triangular faces of the tetrahedron C_i. Let $\mathcal{V}(i)$

denotes the set of tetrahedra that are neighbors of the tetrahedron C_i. Moreover, assume that :

$$\left\{\begin{array}{lcl} \Phi_{H,ij} & \equiv & \Phi_H(\boldsymbol{H}_i, \boldsymbol{H}_j, \mathbf{n}_{ij}) \approx \displaystyle\int_{\partial C_i \cap \partial C_j} N_{\mathbf{n}} \boldsymbol{H} ds \\ \Phi_{E,ij} & \equiv & \Phi_E(\boldsymbol{E}_i, \boldsymbol{E}_j, \mathbf{n}_{ij}) \approx \displaystyle\int_{\partial C_i \cap \partial C_j} N_{\mathbf{n}} \boldsymbol{E} ds \end{array}\right. \tag{43}$$

Note that due to the cell centered finite volume formulation adopted here, the quantities $\Phi_{H,ij}$ and $\Phi_{E,ij}$ stand for elementary fluxes through the interface $\partial C_i \cap \partial C_j$. An implicit finite volume discretization of the Maxwell equations (34) writes as :

$$B_i V_i \frac{W_i^{n+1} - W_i^n}{\Delta t} + \sum_{j \in \mathcal{V}(i)} \Phi_{ij} = 0$$

where $B_i = \mathrm{diag}(\varepsilon_i \mathbb{I}_3, \mu_i \mathbb{I}_3)$ and $\Phi_{ij} = (\Phi_H, -\Phi_E)^t$ defines the flux between the cells i and j. The numerical scheme can also be written as :

$$\left\{\begin{array}{lcl} \varepsilon_i V_i \dfrac{\boldsymbol{E}_i^{n+1} - \boldsymbol{E}_i^n}{\Delta t} & + & \displaystyle\sum_{j \in \mathcal{V}(i)} \Phi_{H,ij}^{n+1/2} = 0 \\ \mu_i V_i \dfrac{\boldsymbol{H}_i^{n+1} - \boldsymbol{H}_i^n}{\Delta t} & - & \displaystyle\sum_{j \in \mathcal{V}(i)} \Phi_{E,ij}^{n+1/2} = 0 \end{array}\right. \tag{44}$$

As in the 1D study, we adopt a centered scheme[7] for the computation of the numerical fluxes Φ_H and Φ_E :

$$\left\{\begin{array}{lcl} \Phi_{H,ij}^{n+1/2} & = & N_{ij} \dfrac{\boldsymbol{H}_i^{n+1/2} + \boldsymbol{H}_j^{n+1/2}}{2} \\ \Phi_{E,ij}^{n+1/2} & = & N_{ij} \dfrac{\boldsymbol{E}_i^{n+1/2} + \boldsymbol{E}_j^{n+1/2}}{2} \end{array}\right. \quad \text{with} \quad \left\{\begin{array}{lcl} \boldsymbol{E}_i^{n+1/2} & = & \dfrac{\boldsymbol{E}_i^n + \boldsymbol{E}_i^{n+1}}{2} \\ \boldsymbol{H}_i^{n+1/2} & = & \dfrac{\boldsymbol{H}_i^n + \boldsymbol{H}_i^{n+1}}{2} \end{array}\right. \tag{45}$$

For what concern the numerical treatment of boundary conditions, we adopt the following approximations :

– for a cell with a face on the metallic boundary $\partial\Omega_m$, the fluxes are computed as :

$$\Phi_{H,im}^{n+1/2} = N_{im} \boldsymbol{H}_i^{n+1/2} \quad \text{and} \quad \Phi_{E,im}^{n+1/2} = 0$$

which could be obtained from the discretized equations by using a fictious cell with $\boldsymbol{E}_j^{n,n+1} = -\boldsymbol{E}_i^{n,n+1}$ and $\boldsymbol{H}_j^{n,n+1} = \boldsymbol{H}_i^{n,n+1}$. The choice for $\Phi_{E,ij}^{n+1/2}$ is clearly a second-order approximation of the condition $\mathbf{n} \times \boldsymbol{E} = 0$, whereas the choice for $\Phi_{H,ij}^{n+1/2}$ is clasically used in FDTD methods.

– for a cell located nearby the absorbing boundary $\partial\Omega_\infty$, we make use of a Steger-Warming type flux decomposition[11] :

$$\Phi_{i\infty}^{n+1} = \begin{pmatrix} \Phi_{H,i\infty}^{n+1/2} \\ -\Phi_{E,i\infty}^{n+1/2} \end{pmatrix} = \begin{pmatrix} (Z_{\mathbf{n}}^{+} D_w \boldsymbol{H})_i + (Z_{\mathbf{n}}^{-} D_w \boldsymbol{H})_\infty \\ (Z_{\mathbf{n}}^{+} D_w \boldsymbol{E})_i + (Z_{\mathbf{n}}^{-} D_w \boldsymbol{E})_\infty \end{pmatrix}$$

and set $(Z_{\mathbf{n}}^{-} D_w \boldsymbol{H})_\infty = (Z_{\mathbf{n}}^{-} D_w \boldsymbol{E})_\infty = 0$. Thus :

$$\begin{aligned} \Phi_{i\infty}^{n+1} = \begin{pmatrix} \Phi_{H,i\infty}^{n+1/2} \\ \\ -\Phi_{E,i\infty}^{n+1/2} \end{pmatrix} &= (Z_{\mathbf{n}}^{+})_i \begin{pmatrix} \varepsilon_i \boldsymbol{E}_i^{n+1/2} \\ \\ \mu_i \boldsymbol{H}_i^{n+1/2} \end{pmatrix} \\ &= \frac{c_i}{2} \begin{pmatrix} -\dfrac{N_{i\infty}^2}{\| \mathbf{n}_{i\infty} \|} & \bar{z}_i N_{i\infty} \\ \\ -z_i N_{i\infty} & -\dfrac{N_{i\infty}^2}{\| \mathbf{n}_{i\infty} \|} \end{pmatrix} \begin{pmatrix} \varepsilon_i \boldsymbol{E}_i^{n+1/2} \\ \\ \mu_i \boldsymbol{H}_i^{n+1/2} \end{pmatrix} \end{aligned}$$

where $N_{i\infty} = N_{n_{i\infty}}$.

3.2 Matrix form

The discrete equations characterizing the implicit finite volume scheme (44) can be re-written as :
- for the cells C_i that are purely internal i.e $\partial C_i \cap (\partial\Omega_m \cup \partial\Omega_\infty) = \emptyset$:

$$\begin{cases} \sigma_i \varepsilon_i \boldsymbol{E}_i^{n+1} + \displaystyle\sum_{j \in \mathcal{V}(i)} N_{ij} \boldsymbol{H}_j^{n+1} = \sigma_i \varepsilon_i \boldsymbol{E}_i^{n} - \sum_{j \in \mathcal{V}(i)} N_{ij} \boldsymbol{H}_j^{n} \\ \sigma_i \mu_i \boldsymbol{H}_i^{n+1} - \displaystyle\sum_{j \in \mathcal{V}(i)} N_{ij} \boldsymbol{E}_j^{n+1} = \sigma_i \mu_i \boldsymbol{H}_i^{n} + \sum_{j \in \mathcal{V}(i)} N_{ij} \boldsymbol{E}_j^{n} \end{cases} \tag{46}$$

with $\sigma_i = \dfrac{4V_i}{\Delta t}$.
For the cells C_i such that $\partial C_i \cap \partial\Omega_m \neq \emptyset$:

$$\begin{cases} \sigma_i \varepsilon_i \boldsymbol{E}_i^{n+1} + \displaystyle\sum_{m \in \mathcal{M}(i)} N_{im} \boldsymbol{H}_i^{n+1} + \sum_{j \in \mathcal{V}(i)} N_{ij} \boldsymbol{H}_j^{n+1} = \sigma_i \varepsilon_i \boldsymbol{E}_i^{n} - \sum_{m \in \mathcal{M}(i)} N_{im} \boldsymbol{H}_i^{n} - \sum_{j \in \mathcal{V}(i)} N_{ij} \boldsymbol{H}_j^{n} \\ \sigma_i \mu_i \boldsymbol{H}_i^{n+1} + \displaystyle\sum_{m \in \mathcal{M}(i)} N_{im} \boldsymbol{E}_i^{n+1} - \sum_{j \in \mathcal{V}(i)} N_{ij} \boldsymbol{E}_j^{n+1} = \sigma_i \mu_i \boldsymbol{H}_i^{n} - \sum_{m \in \mathcal{M}(i)} N_{im} \boldsymbol{E}_i^{n} + \sum_{j \in \mathcal{V}(i)} N_{ij} \boldsymbol{E}_j^{n} \end{cases} \tag{47}$$

where $\mathcal{M}(i)$ denotes the set of (triangular) faces of C_i that lie on $\partial\Omega_m$ and N_{im} is the associated outwards boundary normal.

- for the cells C_i such that $\partial C_i \cap \partial\Omega_\infty \neq \emptyset$:

$$\left\{ \begin{array}{rcl} M^1_{E,ii}\boldsymbol{E}_i^{n+1} + \sum\limits_{j\in\mathcal{V}(i)} N_{ij}\boldsymbol{H}_j^{n+1} & = & P^1_{E,ii}\boldsymbol{E}_i^{n} - \sum\limits_{j\in\mathcal{V}(i)} N_{ij}\boldsymbol{H}_j^{n} \\ M^2_{H,ii}\boldsymbol{H}_i^{n+1} - \sum\limits_{j\in\mathcal{V}(i)} N_{ij}\boldsymbol{E}_j^{n+1} & = & P^2_{H,ii}\boldsymbol{H}_i^{n} + \sum\limits_{j\in\mathcal{V}(i)} N_{ij}\boldsymbol{E}_i^{n} \end{array} \right. \tag{48}$$

where $\mathcal{I}(i)$ denotes the set of (triangular) faces of C_i that lie on $\partial\Omega_\infty$ and :

$$\left\{ \begin{array}{rcl} M^1_{E,ii} & = & \sigma_i\varepsilon_i \mathrm{I}_3 - \sum\limits_{m\in\mathcal{I}(i)} \bar{z}_i \dfrac{N^2_{i\infty}}{\|\mathbf{n}_{i\infty}\|},\ P^1_{E,ii} = \sigma_i\varepsilon_i \mathrm{I}_3 + \sum\limits_{m\in\mathcal{I}(i)} \bar{z}_i \dfrac{N^2_{i\infty}}{\|\mathbf{n}_{i\infty}\|} \\ M^2_{H,ii} & = & \sigma_i\mu_i \mathrm{I}_3 - \sum\limits_{m\in\mathcal{I}(i)} z_i \dfrac{N^2_{i\infty}}{\|\mathbf{n}_{i\infty}\|},\ P^2_{H,ii} = \sigma_i\mu_i \mathrm{I}_3 + \sum\limits_{m\in\mathcal{I}(i)} z_i \dfrac{N^2_{i\infty}}{\|\mathbf{n}_{i\infty}\|} \end{array} \right.$$

A matrix form of eq. (46) is given by :

$$M_{ii}\boldsymbol{W}_i^{n+1} + \sum_{j\in\mathcal{V}(i)} M_{ij}\boldsymbol{W}_j^{n+1} = P_{ii}\boldsymbol{W}_i^{n} + \sum_{j\in\mathcal{V}(i)} P_{ij}\boldsymbol{W}_j^{n} \tag{49}$$

with :

$$\left\{ \begin{array}{rcl} \boldsymbol{W}_i & = & \begin{pmatrix} \boldsymbol{E}_i \\ \boldsymbol{H}_i \end{pmatrix} \\ M_{ii} & = & \begin{pmatrix} \sigma_i\varepsilon_i \mathrm{I}_3 & \mathrm{O}_3 \\ \mathrm{O}_3 & \sigma_i\mu_i \mathrm{I}_3 \end{pmatrix},\ P_{ii} = M_{ii} \\ M_{ij} & = & \begin{pmatrix} \mathrm{O}_3 & N_{ij} \\ -N_{ij} & \mathrm{O}_3 \end{pmatrix},\ P_{ij} = -M_{ij} \end{array} \right.$$

A matrix form of eq. (47) is given by eq. (49) with :

$$\left\{ \begin{array}{rcl} M_{ii} & = & \begin{pmatrix} \sigma_i\varepsilon_i \mathrm{I}_3 & \mathrm{O}_3 \\ \mathrm{O}_3 & \sigma_i\mu_i \mathrm{I}_3 \end{pmatrix} + \sum\limits_{m\in\mathcal{M}(i)} \begin{pmatrix} \mathrm{O}_3 & N_{im} \\ N_{im} & \mathrm{O}_3 \end{pmatrix} \\ P_{ii} & = & \begin{pmatrix} \sigma_i\varepsilon_i \mathrm{I}_3 & \mathrm{O}_3 \\ \mathrm{O}_3 & \sigma_i\mu_i \mathrm{I}_3 \end{pmatrix} - \sum\limits_{m\in\mathcal{M}(i)} \begin{pmatrix} \mathrm{O}_3 & N_{im} \\ N_{im} & \mathrm{O}_3 \end{pmatrix} \\ M_{ij} & = & \begin{pmatrix} \mathrm{O}_3 & N_{ij} \\ -N_{ij} & \mathrm{O}_3 \end{pmatrix} \\ P_{ij} & = & -M_{ij} \end{array} \right.$$

Similarly, a matrix form of eq. (48) is given by eq. (49) with :

$$\left\{ \begin{array}{rcl} M_{ii} & = & \left(\begin{array}{cc} M^1_{E,ii} & \mathrm{O}_3 \\ \mathrm{O}_3 & M^2_{H,ii} \end{array} \right) \\ P_{ii} & = & \left(\begin{array}{cc} P^1_{E,ii} & \mathrm{O}_3 \\ \mathrm{O}_3 & P^2_{H,ii} \end{array} \right) \\ M_{ij} & = & \left(\begin{array}{cc} \mathrm{O}_3 & N_{ij} \\ -N_{ij} & \mathrm{O}_3 \end{array} \right) \\ P_{ij} & = & -M_{ij} \end{array} \right.$$

If we further denote $\mathbf{W}^n = (W_1^n, ..., W_N^n)$, the vector of all the unknowns (where N is the total number of unknowns) we obtain the global representation of the numerical scheme :

$$M\mathbf{W}^{n+1} = P\mathbf{W}^n \tag{50}$$

where M and P are block matrices with the blocks given by the previous equations.

3.3 Theoretical aspects

As in the one-dimensional case, in the following we will prove the energy conservation properties and the well-possedness of the discrete problem.

3.3.1 Energetic considerations

Proposition 3 *The discret electromagnetic energy given by :*

$$\mathcal{E}^n = \frac{1}{2} \sum_{i=1}^{N} V_i \left[\varepsilon_i (\boldsymbol{E}_i^n)^t \cdot \boldsymbol{E}_i^n + \mu_i (\boldsymbol{H}_i^n)^t \cdot \boldsymbol{H}_i^n \right] \tag{51}$$

is decreasing in time, that is $\mathcal{E}^{n+1} \leq \mathcal{E}^n$. If the computational domain doesn't posses absorbing boundaries, this energy remains constant.

Proof By multiplying the first equation of (44) by $\frac{1}{2}(\boldsymbol{E}_i^{n+1} + \boldsymbol{E}_i^n)^t \equiv (\boldsymbol{E}_i^{n+1/2})^t$, the second one by $\frac{1}{2}(\boldsymbol{H}_i^{n+1} + \boldsymbol{H}_i^n)^t \equiv (\boldsymbol{H}_i^{n+1/2})^t$ and summing both equations over the whole set of cells yield :

$$\frac{\mathcal{E}^{n+1} - \mathcal{E}^n}{\Delta t} = \mathcal{T}_{\text{int}} + \mathcal{T}_{\text{met}} + \mathcal{T}_{\text{inf}} \tag{52}$$

where the different terms of eq. (52) refer to summations of elementary computations (i.e elementary fluxes) on cell interfaces (i.e triangular faces). For purely internal interfaces :

$$\begin{aligned}\mathcal{T}_{\text{int}} &= \sum_{\partial C_i \cap \partial C_j \neq \emptyset} \Big[-(\boldsymbol{E}_i^{n+1/2})^t \Phi_{H,ij}^{n+1/2} + (\boldsymbol{H}_i^{n+1/2})^t \Phi_{E,ij}^{n+1/2} \\ &\qquad -(\boldsymbol{E}_j^{n+1/2})^t \Phi_{H,ji}^{n+1/2} + (\boldsymbol{H}_j^{n+1/2})^t \Phi_{E,ji}^{n+1/2} \Big]\end{aligned} \tag{53}$$

Using the expressions (45) together with the relations $N_{ij}^t = -N_{ij}$ and $N_{ji} = -N_{ij}$, the expression (53) can be reduced to :

$$\mathcal{T}_{\text{int}} = \sum_{\partial C_i \cap \partial C_j \neq \emptyset} \Big[(\boldsymbol{H}_i^{n+1/2})^t N_{ij} \boldsymbol{E}_i^{n+1/2} - (\boldsymbol{H}_j^{n+1/2})^t N_{ij} \boldsymbol{E}_j^{n+1/2} \Big] \tag{54}$$

For the faces on the metallic boundary $\partial\Omega_m$, we have :

$$\begin{aligned}\mathcal{T}_{\text{met}} &= \sum_{\partial C_i \cap \partial \Omega_m \neq \emptyset} \Big[-(\boldsymbol{E}_i^{n+1/2})^t \Phi_{H,im}^{n+1/2} + (\boldsymbol{H}_i^{n+1/2})^t \Phi_{E,im}^{n+1/2} \Big] \\ &= \sum_{\partial C_i \cap \partial \Omega_m \neq \emptyset} \Big[-(\boldsymbol{E}_i^{n+1/2})^t N_{im} \boldsymbol{H}_i^{n+1/2} \Big] \\ &= \sum_{\partial C_i \cap \partial \Omega_m \neq \emptyset} (\boldsymbol{H}_i^{n+1/2})^t N_{im} \boldsymbol{E}_i^{n+1/2}\end{aligned} \tag{55}$$

For the faces on the artificial boundary $\partial\Omega_\infty$, we have :

$$\mathcal{T}_{\text{inf}} = \sum_{\partial C_i \cap \partial \Omega_\infty \neq \emptyset} \left[-\left(\frac{\boldsymbol{E}_i^{n+1} + \boldsymbol{E}_i^n}{2} \right)^t \Phi_{H,i\infty}^{n+1/2} + \left(\frac{\boldsymbol{H}_i^{n+1} + \boldsymbol{H}_i^n}{2} \right)^t \Phi_{E,i\infty}^{n+1/2} \right] \tag{56}$$

Let $\mathcal{W}(i)$ be a decomposition of ∂C_i in termes of elementary surfaces (i.e triangular faces). For a purely internal cell, $\mathcal{W}(i) = \mathcal{V}(i)$; in the general case, $\mathcal{W}(i) = \mathcal{V}(i) \cup (\partial C_i \cap \partial\Omega_m) \cup (\partial C_i \cap \partial\Omega_\infty)$. Then, we have :

$$\begin{aligned}\mathcal{S} &= \mathcal{T}_{\text{int}} + \mathcal{T}_{\text{met}} + \sum_{\partial C_i \cap \partial \Omega_\infty \neq \emptyset} \left[\left(\frac{\boldsymbol{H}_i^{n+1} + \boldsymbol{H}_i^n}{4} \right)^t N_{i\infty} \left(\boldsymbol{E}_i^{n+1} + \boldsymbol{E}_i^n \right) \right] \\ &= \sum_{i=1}^{N} \left[\sum_{j \in \mathcal{W}(i)} \left(\frac{\boldsymbol{H}_i^{n+1} + \boldsymbol{H}_i^n}{4} \right)^t N_{ij} \left(\boldsymbol{E}_i^{n+1} + \boldsymbol{E}_i^n \right) \right] \\ &= \sum_{i=1}^{N} \left[\left(\frac{\boldsymbol{H}_i^{n+1} + \boldsymbol{H}_i^n}{4} \right)^t \left(\sum_{j \in \mathcal{W}(i)} N_{ij} \right) \left(\boldsymbol{E}_i^{n+1} + \boldsymbol{E}_i^n \right) \right] = 0\end{aligned}$$

Thus :

$$\frac{\mathcal{E}^{n+1}-\mathcal{E}^{n}}{\Delta t} = \sum_{\partial C_i \cap \partial\Omega_\infty \neq \emptyset} \left[-\left(\frac{\boldsymbol{E}_i^{n+1}+\boldsymbol{E}_i^{n}}{2}\right)^t \left(\Phi_{H,i\infty}^{n+1/2} - N_{i\infty}\frac{\boldsymbol{H}_i^{n+1}+\boldsymbol{H}_i^{n}}{2}\right) + \left(\frac{\boldsymbol{H}_i^{n+1}+\boldsymbol{H}_i^{n}}{2}\right)^t \Phi_{E,i\infty}^{n+1/2} \right] \tag{57}$$

By replacing the fluxes we get :

$$\begin{aligned}
\frac{\mathcal{E}^{n+1}-\mathcal{E}^{n}}{\Delta t} &= \sum_{\partial C_i \cap \partial\Omega_\infty \neq \emptyset} \left[-\left(\frac{\boldsymbol{E}_i^{n+1}+\boldsymbol{E}_i^{n}}{4}\right)^t \left(-\bar{z}_i \frac{N_{i\infty}^2}{\parallel \mathbf{n}_{i\infty} \parallel}\boldsymbol{E}_i^{n+1/2} - N_{i\infty}\boldsymbol{H}_i^{n+1/2}\right) + \left(\frac{\boldsymbol{H}_i^{n+1}+\boldsymbol{H}_i^{n}}{4}\right)^t \left(N_{i\infty}\boldsymbol{E}_i^{n+1/2} + z_i \frac{N_{i\infty}^2}{\parallel \mathbf{n}_{i\infty} \parallel}\boldsymbol{H}_i^{n+1/2}\right) \right] \\
&= \sum_{\partial C_i \cap \partial\Omega_\infty \neq \emptyset} \left[\frac{\bar{z}_i}{2 \parallel \mathbf{n}_{i\infty} \parallel} (\boldsymbol{E}_i^{n+1/2})^t N_{i\infty}^2 \boldsymbol{E}_i^{n+1/2} + \frac{z_i}{2 \parallel \mathbf{n}_{i\infty} \parallel} (\boldsymbol{H}_i^{n+1/2})^t N_{i\infty}^2 \boldsymbol{H}_i^{n+1/2} \right] \\
&+ \sum_{\partial C_i \cap \partial\Omega_\infty \neq \emptyset} \left[(\boldsymbol{E}_i^{n+1/2})^t N_{i\infty} \boldsymbol{H}_i^{n+1/2} + (\boldsymbol{H}_i^{n+1/2})^t N_{i\infty} \boldsymbol{E}_i^{n+1/2} \right] \\
&= \sum_{\partial C_i \cap \partial\Omega_\infty \neq \emptyset} \frac{1}{2 \parallel \mathbf{n}_{i\infty} \parallel} \left[\bar{z}_i (\boldsymbol{E}_i^{n+1/2})^t N_{i\infty}^2 \boldsymbol{E}_i^{n+1/2} + z_i (\boldsymbol{H}_i^{n+1/2})^t N_{i\infty}^2 \boldsymbol{H}_i^{n+1/2} \right] \leq 0
\end{aligned} \tag{58}$$

since the matrix $N_{i\infty}^2$ is symmetric negative definite (a simple calculation shows that its eigenvalues are 0 and $- \parallel \mathbf{n}_{i\infty} \parallel^2$). Therefore the total energy is decreasing $\mathcal{E}^{n+1} \leq \mathcal{E}^n$. ■

3.3.2 Inversibility of the implicit matrix

Proposition 4 *The matrix M given by (50) is positive definite and therefore invertible.*

Proof Using the structure of the matrix M, we can show that it is a positive definite matrix, that is for any $\mathbf{X} = (X^1, X^2)^t \in \mathbb{R}^{6N}$ $\mathbf{X}^t M \mathbf{X} > 0$ which will prove the invertibility of M. First we notice that all the matrices N_{ij}, N_{im}, $N_{i\infty}$ are skew-symmetric and therefore for each pair of vectors $\mathbf{y}$ and $\mathbf{z}$ we have $\mathbf{y}^t N_{ij} \mathbf{z} + \mathbf{z}^t N_{ij} \mathbf{y} = 0$. The same property yields for N_{im} and $N_{i\infty}$. Thus :

$$
\begin{aligned}
\mathbf{X}^t M \mathbf{X} &= \sum_{i=1}^{N} \mathbf{X}_i^t M_{ii} \mathbf{X}_i + \sum_{1 \le i \ne j \le N} \mathbf{X}_i^t M_{ij} \mathbf{X}_j \\
&= \sum_{i=1}^{N} \{ \mathbf{X}_i^t \begin{pmatrix} \sigma_i \varepsilon_i \mathrm{I}_3 & \mathrm{O}_3 \\ \mathrm{O}_3 & \sigma_i \mu_i \mathrm{I}_3 \end{pmatrix} \mathbf{X}_i + \sum_{m \in \mathcal{M}(i)} \left((\mathbf{X}_i^1)^t N_{im} \mathbf{X}_i^2 + (\mathbf{X}_i^2)^t N_{im} \mathbf{X}_i^1 \right) + \\
&\qquad \sum_{m \in \mathcal{I}(i)} \left(-\frac{\bar{z}_i}{\|\mathbf{n}_{i\infty}\|} (\mathbf{X}_i^1)^t N_{i\infty}^2 \mathbf{X}_i^1 - \frac{z_i}{\|\mathbf{n}_{i\infty}\|} (\mathbf{X}_i^2)^t N_{i\infty}^2 \mathbf{X}_i^2 \right) \} \\
&+ \sum_{1 \le i \ne j \le N} \left[-(\mathbf{X}_i^2)^t N_{ij} \mathbf{X}_j^1 + (\mathbf{X}_i^1)^t N_{ij} \mathbf{X}_j^2 \right] \\
&= \sum_{i=1}^{N} \{ \sigma_i \varepsilon_i (\mathbf{X}_i^1)^t \mathbf{X}_i^1 + \sigma_i \mu_i (\mathbf{X}_i^2)^t \mathbf{X}_i^2 + \\
&\qquad \frac{1}{\|\mathbf{n}_{i\infty}\|} \sum_{m \in \mathcal{I}(i)} \left[-\bar{z}_i (\mathbf{X}_i^1)^t N_{i\infty}^2 \mathbf{X}_i^1 - z_i (\mathbf{X}_i^2)^t N_{i\infty}^2 \mathbf{X}_i^2 \right] \} \\
&+ \sum_{i=1}^{N} \sum_{m \in \mathcal{M}(i)} \left[(\mathbf{X}_i^1)^t N_{im} \mathbf{X}_i^2 + (\mathbf{X}_i^2)^t N_{im} \mathbf{X}_i^1 \right] \\
&+ \sum_{1 \le i < j \le N} \left[-(\mathbf{X}_i^2)^t N_{ij} \mathbf{X}_j^1 + (\mathbf{X}_i^1)^t N_{ij} \mathbf{X}_j^2 + (\mathbf{X}_j^2)^t N_{ij} \mathbf{X}_i^1 - (\mathbf{X}_j^1)^t N_{ij} \mathbf{X}_i^2 \right] \\
&= \sum_{i=1}^{N} \{ \sigma_i \varepsilon_i (\mathbf{X}_i^1)^t \mathbf{X}_i^1 + \sigma_i \mu_i (\mathbf{X}_i^2)^t \mathbf{X}_i^2 + \\
&\qquad \frac{1}{\|\mathbf{n}_{i\infty}\|} \sum_{m \in \mathcal{I}(i)} \left[-\bar{z}_i (\mathbf{X}_i^1)^t N_{i\infty}^2 \mathbf{X}_i^1 - z_i (\mathbf{X}_i^2)^t N_{i\infty}^2 \mathbf{X}_i^2 \right] \}
\end{aligned}
$$

Thus, for $\mathbf{X} \neq 0$, we have that $\mathbf{X}^t M \mathbf{X} > 0$ since the matrix $-N_{i\infty}^2$ is positive semi-definite. Therefore M is positive definite and thus invertible. ■

3.4 Numerical results

We present here preliminary results using a model 3D problem consisting in the numerical simulation of the time evolution of an eigenmode in a metallic cubic cavity of unitary length. We consider the (0,1,1) mode oscillating at a frequency of 131 Mhz. A regular tetrahedral mesh is obtained by subdividing the cells of finite difference grid. Comparisons between the exact solution and the one provided by the proposed IFVTD method are shown on figures 9 to 11 for CFL numbers respectively equal to 1, 5 and 10. As expected, the dispersion error introduced by the IFVTD method increases with the duration of the simulation but this test

case certainly represent one of the most challengling one (in terms of accuracy) for implicit time integration schemes such as the one considered here.

3.5 Future works

There are several possible sequels to the work presented here, some of them being currently under investigation :

- extension to Discontinuous Galerkin (DG) formulations. We are currently extending the proposed IFVTD method to the DG method based on linear interpolation inside each tetrahedron, previously proposed for the time domain Maxwell equations[6].
- higher-order implicit time integration methods. The Crank-Nicolson adopted here is second-order accurate. However, it is a also the source of a temporal dispersion error whose adverse effect increases with the CFL number. It is clear that one should seek for more accurate implicit time integration schemes.
- hybrid explicit/implicit finite volume and DG methods. Ideally, we expect that an implicit time integration scheme will be particularly valuable when used locally, in zones where the tetrahedal mesh is refined. Then, the challenge is to construct stable hybrid explicit/implicit methods with a CFL (i.e. a time step) varying is space.

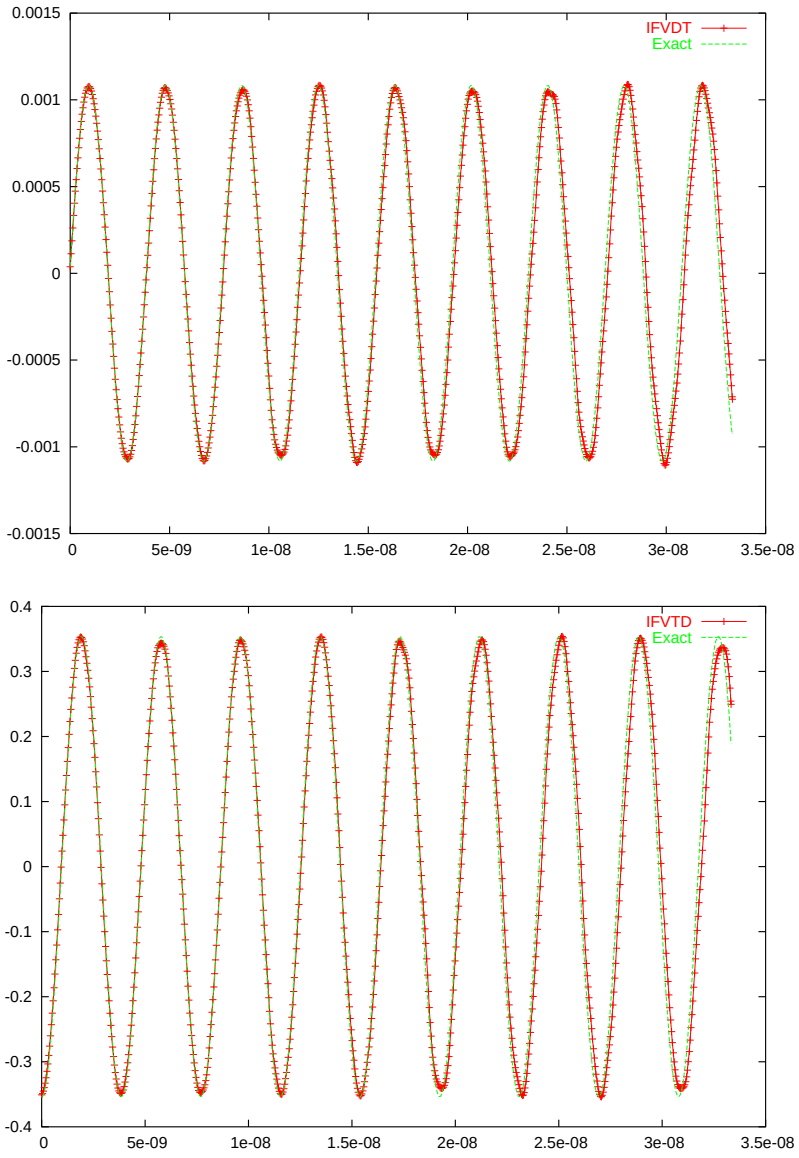

FIG. 9 – Comparison beetween the exact and numerical solution CFL=1 : E_z and H_y

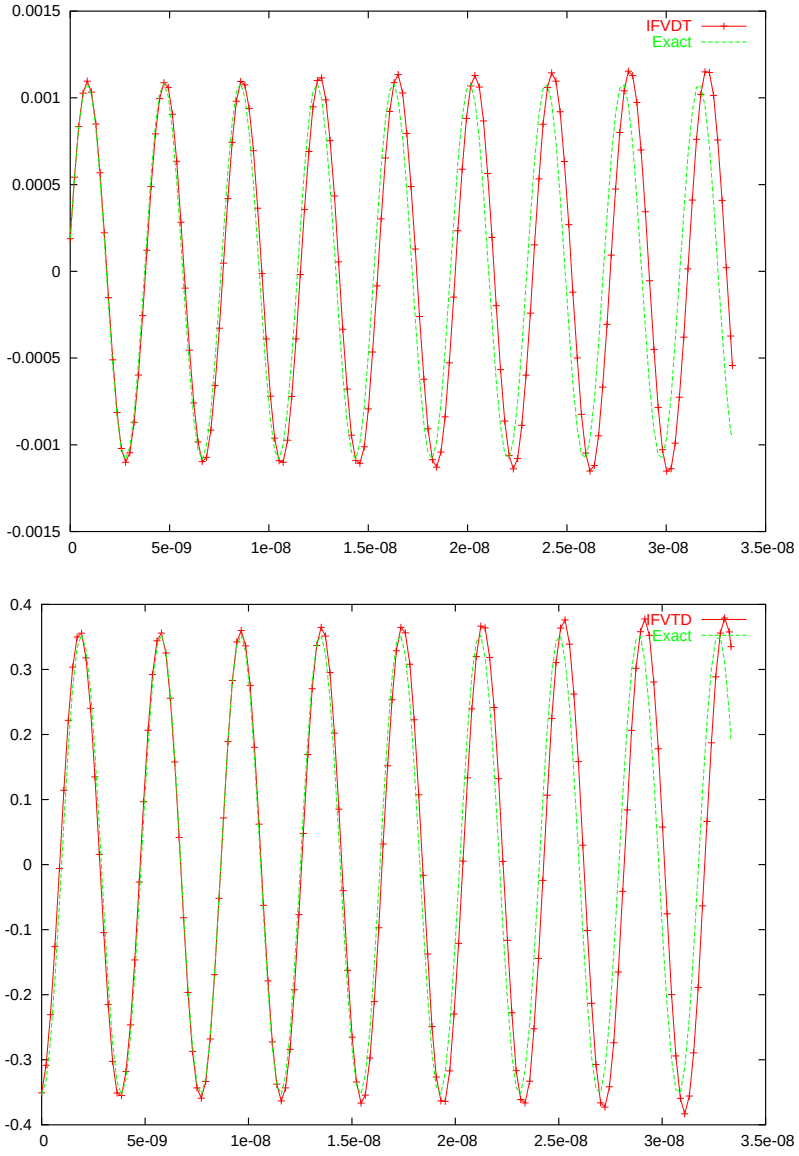

FIG. 10 – Comparison beetween the exact and numerical solution CFL=5 : E_z and H_y

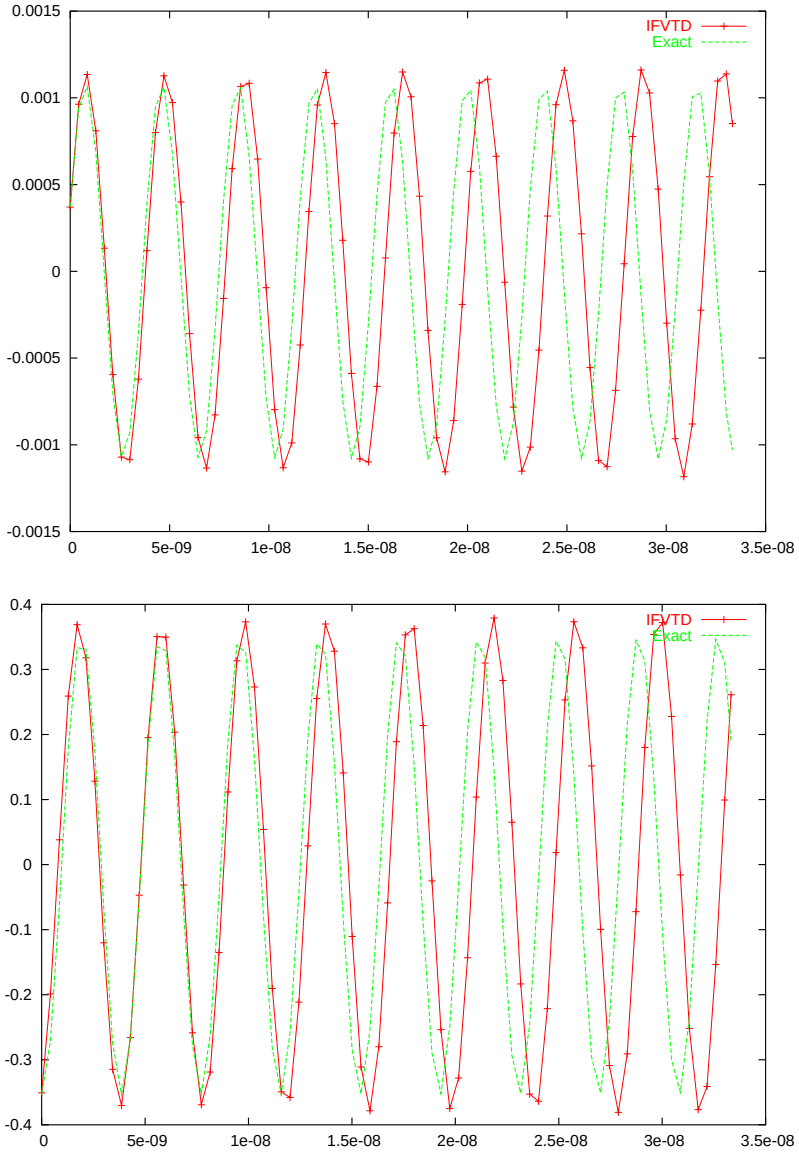

FIG. 11 – Comparison beetween the exact and numerical solution CFL=10 : E_z and H_y

Références

[1] P. Bonnet. *Résolution des équations de Maxwell instationnaires et harmoniques par une technique de volumes finis. Application à des problèmes de compatibilité électromagnétique.* PhD thesis, ONERA, 2000.

[2] J.P. Cioni, L. Fezoui, L. Anne, and F. Poupaud. A parallel FVTD Maxwell solver using 3D unstructured meshes. In *13th Annual Review of Progress in Applied Computational Electromagnetics (PIERS)*, pages 359–365, 1997.

[3] L. Fezoui, S. Lanteri, S. Lohrengel, and S. Piperno. Convergence and stability of a discontinuous Galerkin time-domain method for the 3D heterogeneous Maxwell equations on unstructured meshes. *ESAIM : Modél. Math. Anal. Numér.*, 2005. to appear.

[4] P. Helluy. *Rśolution numérique des équations de Maxwell harmoniques par une méthode d'éléments finis discontinus.* PhD thesis, Ecole Nationale Supérieure de l'Aéronautique, 1994.

[5] S. Piperno. l^2-stability of the upwind first order finite volume scheme for the Maxwell equations in two and three dimensions on arbitrary unstructured meshes. *RAIRO : Modél. Math. Anal. Numér.*, 34 :139–158, 2000.

[6] S. Piperno and L. Fezoui. A centered discontinuous Galerkin finite volume scheme for the 3D heterogeneous Maxwell equations on unstructured meshes. INRIA Research Report No. 4733, 2003.

[7] S. Piperno, M. Remaki, and L. Fezoui. A nondiffusive finite volume scheme for the three-dimensional Maxwell's equations on unstructured meshes. *SIAM J. Num. Anal.*, 39(6) :2089–2108, 2002.

[8] M. Remaki. A new finite volume scheme for solving Maxwell's system. *COMPEL*, 19 :913–931, 2000.

[9] J.S. Shang and R.M. Fithen. A comparative study of characteristic-based algorithms for the Maxwell equations. *J. Comput. Phys.*, 125 :378–394, 1996.

[10] V. Shankar, W. Hall, and A. Mohammadian. A time-domain differential solver for electromagnetic problems. In *IEE*, volume 77, pages 709–721, 1989.

[11] J. Steger and R. F. Warming. Flux vector splitting for the inviscid gas dynamic with applications to finite difference methods. *J. of Comp. Phys.*, 40 :263–293, 1981.

[12] K.S. Yee. Numerical solution of initial boundary value problems involving Maxwell's equations in isotropic media. *IEEE Trans. Antennas and Propagation*, AP-16 :302–307, 1966.

Unité de recherche INRIA Sophia Antipolis
2004, route des Lucioles - BP 93 - 06902 Sophia Antipolis Cedex (France)

Unité de recherche INRIA Futurs : Parc Club Orsay Université - ZAC des Vignes
4, rue Jacques Monod - 91893 ORSAY Cedex (France)
Unité de recherche INRIA Lorraine : LORIA, Technopôle de Nancy-Brabois - Campus scientifique
615, rue du Jardin Botanique - BP 101 - 54602 Villers-lès-Nancy Cedex (France)
Unité de recherche INRIA Rennes : IRISA, Campus universitaire de Beaulieu - 35042 Rennes Cedex (France)
Unité de recherche INRIA Rhône-Alpes : 655, avenue de l'Europe - 38334 Montbonnot Saint-Ismier (France)
Unité de recherche INRIA Rocquencourt : Domaine de Voluceau - Rocquencourt - BP 105 - 78153 Le Chesnay Cedex (France)

Éditeur
INRIA - Domaine de Voluceau - Rocquencourt, BP 105 - 78153 Le Chesnay Cedex (France)
http://www.inria.fr
ISSN 0249-6399